

Thickness dependence of electron-electron interactions in topological p - n junctions

Dirk Backes,^{1,2,*} Danhong Huang,³ Rhodri Mansell,¹ Martin Lanius,⁴ Jörn Kampmeier,⁴ David Ritchie,¹ Gregor Mussler,⁴ Godfrey Gumbs,⁵ Detlev Grützmacher,⁴ and Vijay Narayan^{1,†}

¹*Cavendish Laboratory, University of Cambridge,
J. J. Thomson Avenue, Cambridge CB3 0HE, United Kingdom*

²*Department of Physics, Loughborough University,
Epinal Way, Loughborough LE11 3TU, United Kingdom*

³*Air Force Research Laboratory, Space Vehicles Directorate,
Kirtland Air Force Base, New Mexico 87117, USA*

⁴*Peter Grünberg Institute (PGI-9), Forschungszentrum Jülich, 52425 Jülich, Germany*

⁵*Department of Physics and Astronomy,
Hunter College of the City University of New York,
695 Park Avenue, New York, New York 10065, USA*

(Dated: March 17, 2022)

Abstract

Electron-electron interactions in topological p - n junctions consisting of vertically stacked topological insulators are investigated. n -type Bi_2Te_3 and p -type Sb_2Te_3 of varying relative thicknesses are deposited using molecular beam epitaxy and their electronic properties measured using low-temperature transport. The screening factor is observed to decrease with increasing sample thickness, a finding which is corroborated by semi-classical Boltzmann theory. The number of two-dimensional states determined from electron-electron interactions is larger compared to the number obtained from weak-antilocalization, in line with earlier experiments using single layers.

PACS numbers: 73.20.-r, 73.25.+i, 73.50.-h

I. INTRODUCTION

Topological insulators are fascinating materials with conducting surfaces, harboring electronic states with a Dirac-like bandstructure¹. Large spin-orbit interaction together with time reversal symmetry cause the topological nature of these surface states (TSS), manifesting itself in the suppression of backscattering and leading to the weak-antilocalization effect (WAL) and to spin-momentum coupling. Furthermore, magnetic topological insulators exhibit the quantum anomalous Hall (QAH) effect²⁻⁴, characterized by dissipationless chiral currents. These properties of topological insulators have attracted great attention because of their potential applications in energy-efficient electronics and quantum computing.

The analysis of the topological properties is complicated by the non-zero conductivity of the bulk⁵⁻⁷, which often dominates the overall transport characteristics. Several methods have been devised to suppress the bulk contribution, such as doping⁸⁻¹¹, gating^{6,12-14}, and reducing the thickness of the layer¹⁵. A relatively unexplored but elegant method is to combine an electron and hole dominated material to form a p - n junction, and thus creating a depletion layer at the interface¹⁶⁻¹⁸.

The π -Berry phase of the Dirac fermions gives rise to quantum corrections of the conductivity, with a magnetic field and temperature dependence resembling the WAL effect. By analyzing of the WAL in topological p - n junctions the transport through TSS and bulk states was disentangled¹⁸. Additional modifications of the conductivity are caused by electron-electron interactions (EEI), originating from an effective decrease of the electron density at the Fermi level¹⁹⁻²². The combined study of both WAL and EEI can reveal information about spin (EEI) and orbital (WAL) part of the electron wave function to transport²³.

Especially the number of 2D states n is of utmost interest, since it can provide evidence of the topological nature of a TI^{24,25}. By careful observation of either the WAL or EEI, a value for n can be gained²⁶⁻³⁷. It turns out that in single layer TI, n_{EEI} tends to be larger than n_{WAL} ^{26,27,29-32,35-37} (see Fig. 1 and Tab.II). It seems that surface states on the top and bottom contribute independently to EEI but that, under certain circumstances, they appear to be coupled when the WAL effect is concerned. The physical origin of this coupling effect remains elusive. Predominantly in very thin layers only one 2D state contributes to WAL^{30,33-35,37}. Thicker films tend to be decoupled when WAL is concerned and therefore exhibit a higher number of 2D-channels^{28,31,36,37}. Microflakes²⁹ and hot wall epitaxy deposited

layers²⁷ are exceptions where coupling effects can be observed even at thicknesses > 60 nm. A combined study of the WAL and EEI in TI-multilayers is entirely missing.

In the following, we present the first investigation of the interplay of WAL and EEI in topological p - n junctions. Conductivity corrections are measured at temperatures < 10 K as a function of temperature, magnetic field and sample thickness. The conductivity correction are used to find the number of 2D channels contributing to either EEI or WAL. Finally, a semiclassical Boltzmann theory is derived to understand the thickness dependence of the conductivity corrections due to EEI.

II. EXPERIMENT

The $\text{Bi}_2\text{Te}_3/\text{Sb}_2\text{Te}_3$ -bilayers (BST) were grown using molecular beam epitaxy (MBE). Details of the MBE sample preparation can be found in Ref. 17. The bottom Bi_2Te_3 -layer was $t_{\text{BiTe}} = 6$ nm and the top Sb_2Te_3 -layers was 6.6 nm (BST6), 7.5 nm (BST7), 15 nm (BST15), and 25 nm (BST25) thick, respectively. The films were patterned into Hall bars which were $200 \mu\text{m}$ wide and $1000 \mu\text{m}$ long. Transport in these samples was measured in a He-3 cryostat at temperature down to 300 mK while a perpendicular magnetic field could be applied using a superconductive magnet.

III. RESULTS

In Fig. 2 the sheet resistance R_s during cooldown is shown for all sample thicknesses. Metallic behavior is dominant, except for the thinnest samples, BST6 and 7, which are insulating between room temperature and 200 K, where they become metallic. At base temperature (300 mK) all samples are insulating, with the transition temperature between the metallic and insulating phase, T^* , found to be between 7 to 11 K, depending on the sample thickness (see insert in Fig. 2(a)).

The temperature range below T^* is explored in more detail in Fig. 3 for each sample thickness. The temperature was increased in small steps starting at base temperature of 300 mK, taking care for the temperature to stabilize. An external magnetic field was swept between 0 and 0.5 T at each temperature step. Both longitudinal and transverse resistance were recorded from which the conductivity could be calculated. Only one field loop needed

Ref.	Sample	Method	t/nm
Roy et al. ³⁰	BiTe	MBE	4
Wang et al. ³⁷	BiSe	SP	6-108
Jing et al. ³³	BiSe	MBE	10
Trivedi et al. ³⁴	BiTeS	Flakes	10
Kuntsevich et al. ³⁵	BiSe films	MBE	10-18
Sahu et al. ³⁶	BiSe films	SP	20
Takagaki et al. ²⁸	SbTe films	MBE	21
Takagaki et al. ³¹	SbTe	MBE	22
Chiu et al. ²⁹	BiTe	Flakes	65
Takagaki et al. ²⁷	Cu-doped BiSe	HWE	80

TABLE I. Sample details of experiments reporting both on WAL and EEI. Most results are reported on thin films grown by molecular beam epitaxy (MBE) and sputtering (sp) and a few by hot wall epitaxy (HTW) and on microflakes.

to be taken since the noise level was low.

IV. DISCUSSION

EEI originate from pairing of electrons at the Fermi energy and lead to a decrease in the carrier density, which in turn leads to a reduction of the conductivity. As can be seen in Fig. 3, the correction to conductivity due to EEI sets in below a transition temperature and exhibits a well-defined temperature dependence, given by¹⁹

$$\delta\sigma(T) = -\frac{e}{\pi h}n \left(1 - \frac{3}{4}F\right) \ln\left(\frac{T}{T^*}\right) \quad (1)$$

where n is the number of 2D channels, F the screening factor, and T^* the transition temperature. By applying Eq. 1 to the measured conductivity in Fig. 3 using T^* (see insert in Fig. 2(a)), we obtain $f = n(1 - 3/4 * F)$ from the slope of the temperature dependence.

The overall change of the conductivity correction between base and transition temperature, $\delta\sigma_{5\text{K}} - \delta\sigma_{300\text{mK}}$, increases with sample thickness (see Fig. 4(a)).

Fig. 4(b) shows the change of f when a magnetic field is applied perpendicular to the sample. The value of f is smaller than 1 without magnetic field but rises to values close or

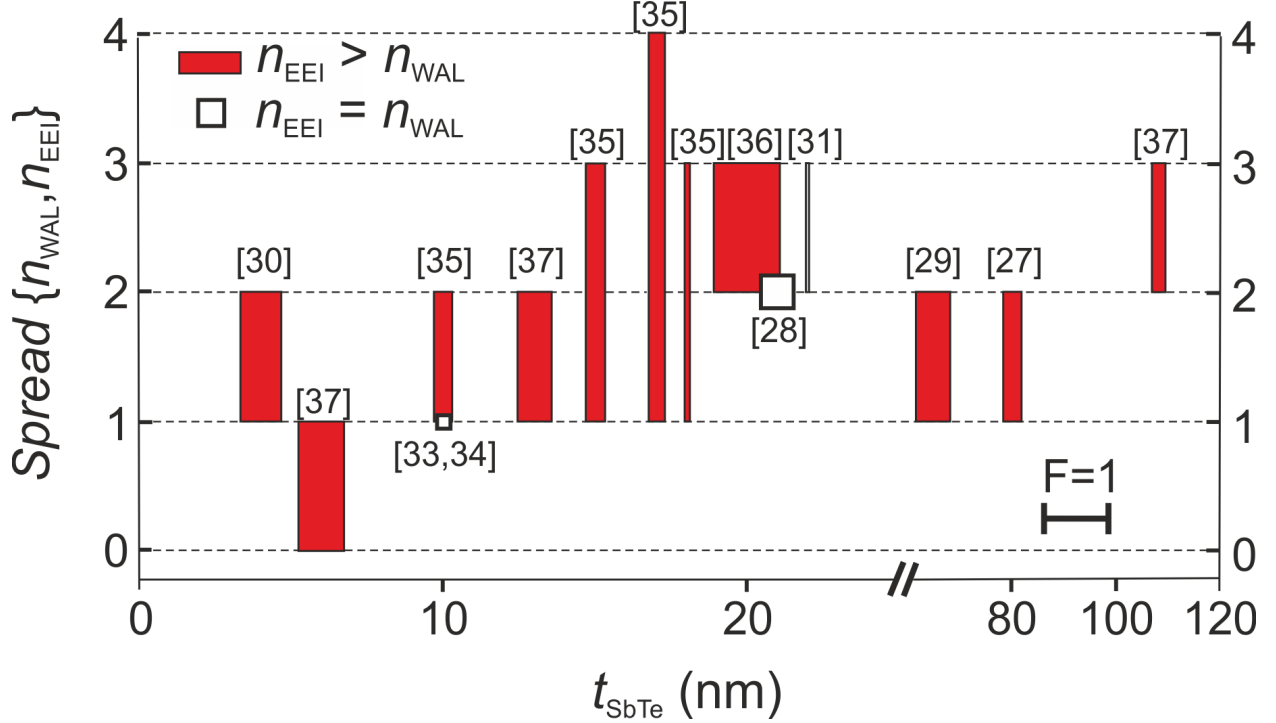


FIG. 1. Comparison of the number of 2D channels from WAL (n_{WAL}) and EEI (n_{EEI}) as a function of the layer thickness. The values are taken from literature, with the references given in brackets. The bars indicate the spread between n_{EEI} (top) and n_{WAL} (bottom). Squares indicate experiments where $n_{\text{EEI}} = n_{\text{WAL}}$. The widths of the bars are proportional to the screening factor F (see scale bar in the bottom right).

above 1 at fields ≈ 0.2 T. This abrupt change reflects the disruption of phase coherence due to the magnetic field, impacting WAL. At fields > 0.2 T, where WAL has disappeared¹⁸, any change in conductivity can be attributed to EEI. f saturates above this field (see Fig. 4(b)) and is employed to investigate the underlying EEI it originates from. The screening parameter F can be inferred from f if n , the number of 2D states is known. F can attain values between 0 (no screening) and 1 (strong screening). This condition cannot be fulfilled when f is larger than 1 and $n = 1$. Thus, to obtain an F within the allowed range from our experimental results²⁷ we assume that $n > 1$ (see Fig. 4(c)).

For $n = 2$ the screening factor F decreases with thickness, from 0.73 for BST6 to 0.5 for BST25 (see Fig. 4(c)). It cannot be excluded that $n > 2$ but although the values of F differ, the thickness dependence remains unchanged. This goes hand-in-hand with a similar thickness-dependent increase of the conductivity correction, since weaker screening means

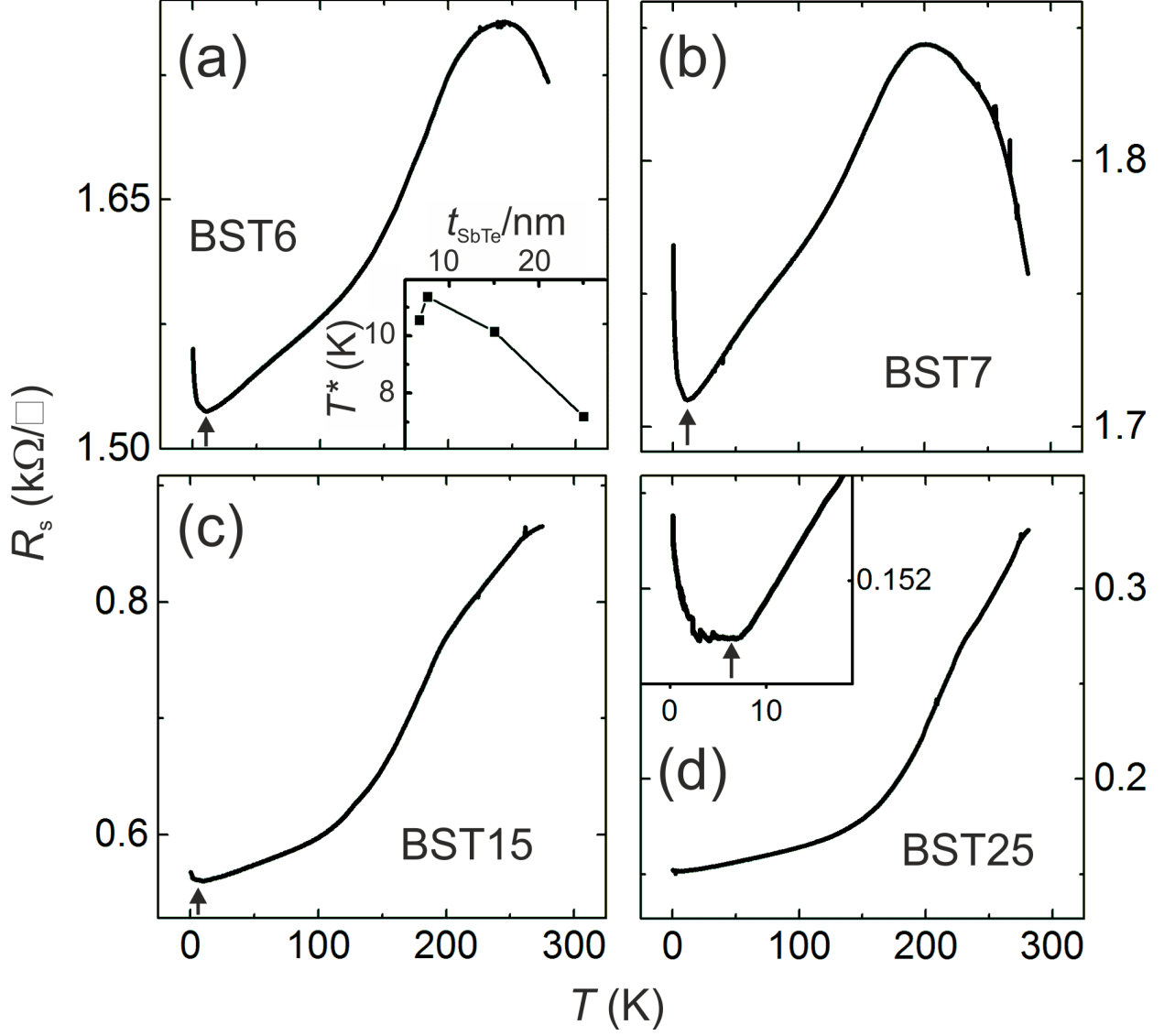


FIG. 2. (a)-(d) Sheet resistance R_s dependence on temperature for four different samples. The arrows indicate the transition temperature T^* . Insert in (a) Transition temperature T^* dependence on thickness of the Sb_2Te_3 -layer

stronger EEI, hence larger $\delta\sigma$. In single layers, both a decrease^{35,37} as well as an increase³⁴ of F with increasing thickness have been reported. The increase was attributed to a stronger screening due to the bulk states in thicker samples³⁴.

To explain our results in light of these contradicting earlier observations, we derived a semi-classical Boltzmann theory for the topological p - n junctions. The total conductivity (see Eqns. C18 and C19 in the Supplement³⁸ for its derivation) is given by

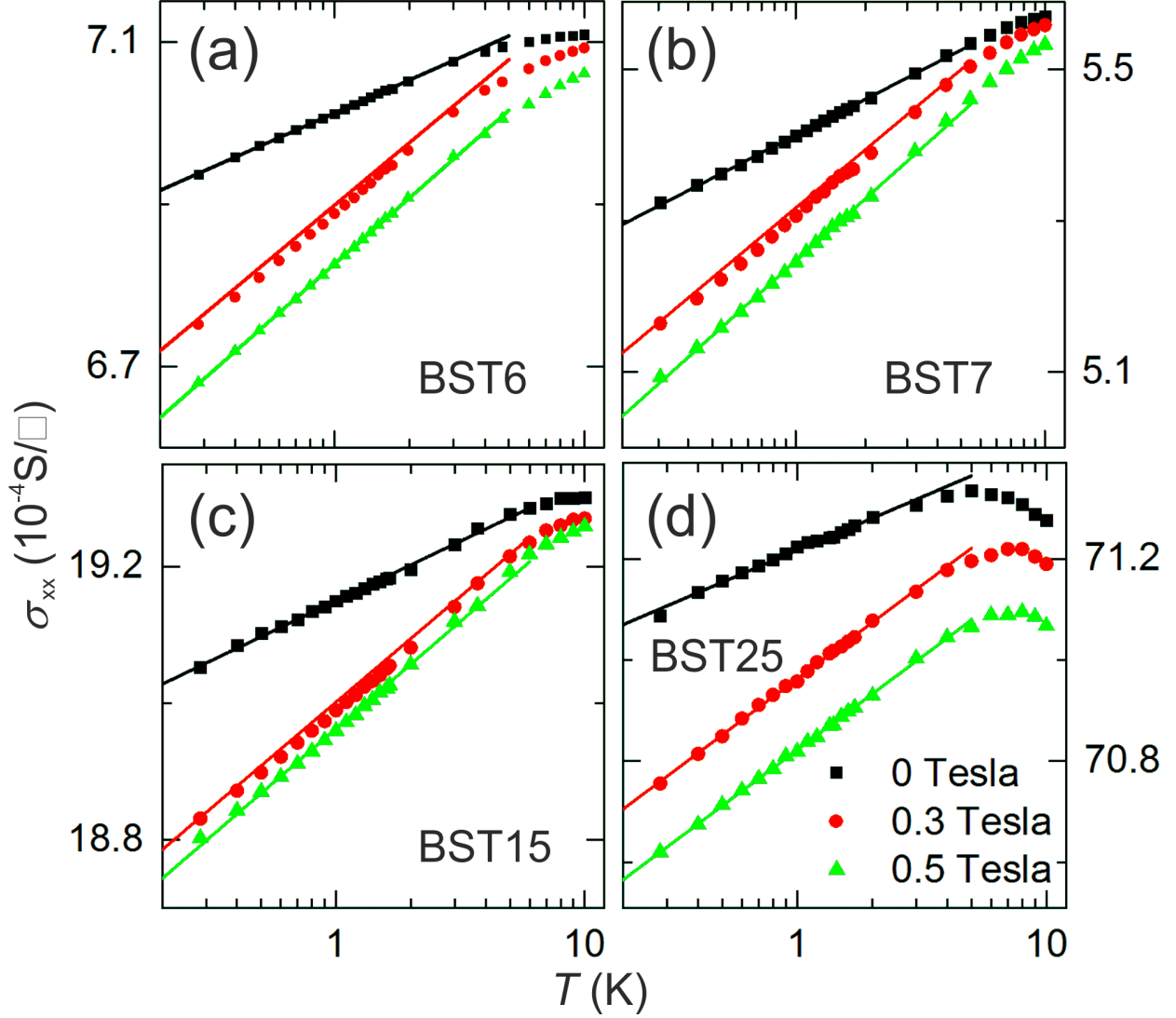


FIG. 3. (a) - (d) Conductivity of four different samples at low temperature for three different perpendicular magnetic fields. Using a logarithmic scale for the temperature, the linear regions are fitted using Eqn. 1 (straight lines). The magnetic field leads to a change of slope, from which the screening and number of 2D channels can be derived.

$$\begin{aligned}
\vec{\sigma}_{\text{tot}}(\mathbf{B}) = & e \hat{\mu}_v^{\parallel}(\mathbf{B}) N_A A_h \left[(L_A - W_p) + \int_0^{W_p} dz \exp\left(-\frac{\beta e \bar{\mu}_h N_A}{2\epsilon_0 \epsilon_r D_h} z^2\right) \right] - e \hat{\mu}_c^{\parallel}(\mathbf{B}) N_D A_e \\
& \times \left[(L_D - W_n) + \int_0^{W_n} dz \exp\left(-\frac{\beta e \bar{\mu}_e N_D}{2\epsilon_0 \epsilon_r D_e} z^2\right) \right] + e \hat{\mu}_s^{\pm}(\mathbf{B}) \left(\frac{\alpha_0 \Delta_0}{2\pi \hbar^2 v_F^2} \right) (L_A - L_0) A_s
\end{aligned} \quad (2)$$

where $A_s = \tau_s / \tau_{\text{sp}}$ and $A_{e,h} = \tau_{e,h} / \tau_{\text{p}(e,h)}$. τ_s and $\tau_{e,h}$ are the energy relaxation and τ_{sp} and

$\tau_{p(e,h)}$ the momentum relaxation time of the surface and bulk, respectively. $L_{A,D}$, $N_{A,D}$, $\bar{\mu}_{h,e}$, $W_{p,n}$, and $D_{h,e}$ are thickness, electron density, mobility, range of depletion zone and diffusion coefficient of the acceptor (donator) layer, respectively. v_F is the Fermi velocity of the surface states which are allowed to have a small band gap Δ_0 due to hybridization at small thicknesses. α_0 and L_0 are constants to be determined experimentally. The surface mobility is

$$\vec{\mu}_s(\mathbf{B}) = \frac{\mu_1}{1 + \mu_1^2 B^2} \begin{bmatrix} 1 & \mu_1 B \\ -\mu_1 B & 1 \end{bmatrix}, \quad (3)$$

with $\mu_1 = e\tau_{sp}v_F^2/\Delta_0 = e\tau_{sp}v_F^2/2k_B T_0$. For weak magnetic field, we have $\mu_1 B \ll 1$, $\mu_{xx} = \mu_{yy} = \mu_1$ and $\mu_{xy} = -\mu_{yx} = \mu_{21} B$.

When $B \rightarrow 0$ the conductance correction (see Eq. C20 in the Supplement³⁸) is given by

$$\begin{aligned} \delta\sigma(T_e, u_s) &\equiv \sigma_{\text{tot}}(T_e, u_s) - \sigma_{\text{tot}}^{(0)}(T_e, u_s) \\ &= -\mu_0^s \left(\frac{\alpha_0 \Delta_0}{2\pi\hbar^2 v_F^2} \right) (L_A - L_0) \left[\frac{\tau_0^s(T_e, u_s)}{\tau_0^s(T_e, u_s) + \tau_{\text{pair}}^s(T_e, u_s)} \right] \\ &\approx -\sigma_0^s \left[\frac{\tau_0^s(T_e, u_s)}{\tau_{\text{pair}}^s(T_e, u_s)} \right], \end{aligned} \quad (4)$$

where $\mu_0^s = e\tau_0^s v_F^2/\Delta_0 = e\tau_0^s v_F^2/2k_B T^*$, σ_0^s and τ_0^s are the mobility, conductivity and energy-relaxation time, respectively, of surface electrons in the absence of EEI.

Here, $\tau_{\text{pair}}^s(T_e, u_s)$ is the additional electron-electron pair scattering contribution to the inverse energy relaxation time (see Eq. C16 and C17 in the Supplement³⁸), given by

$$\begin{aligned} \frac{1}{\tau_{\text{pair}}^s(T_e, u_s)} &= \frac{1}{n_0 \mathcal{A}} \sum_{\mathbf{k}_{\parallel}} \frac{f_{\mathbf{k}_{\parallel}}^s}{\tau_{\text{pair}}^s(\mathbf{k}_{\parallel})} \approx \frac{1}{16\pi^4 \hbar n_0} \left(\frac{e^2}{2\epsilon_0 \epsilon_b} \right)^2 \\ &\times \int_{90}^{1/\delta_s} \frac{dq_{\parallel}}{q_{\parallel}} \left\{ 1 - \left(\frac{e^2 q_{\parallel}}{2\epsilon_0 \epsilon_b} \right) \frac{32k_B T^*}{\pi\hbar^2 \Gamma_0^2} \left(\frac{T^*}{T_e} \right) D \right\} \int d^2 \mathbf{k}_{\parallel} f_{\mathbf{k}_{\parallel}}^s \\ &\times \int d^2 \mathbf{k}'_{\parallel} \left[f_{\mathbf{k}'_{\parallel}}^s (1 - f_{\mathbf{k}_{\parallel}}^s) (1 - f_{\mathbf{k}'_{\parallel}+}^s) + f_{\mathbf{k}_{\parallel}}^s f_{\mathbf{k}'_{\parallel}+}^s (1 - f_{\mathbf{k}'_{\parallel}}^s) \right] \\ &\times \frac{\Gamma_0/\pi}{(\epsilon_{\mathbf{k}_{\parallel}}^s + \epsilon_{\mathbf{k}'_{\parallel}}^s - \epsilon_{\mathbf{k}_{\parallel}-}^s - \epsilon_{\mathbf{k}'_{\parallel}+}^s)^2 + \Gamma_0^2}, \end{aligned} \quad (5)$$

where

$$f_{\mathbf{k}_{\parallel}}^s \approx \frac{2\pi\hbar^2 v_F^2 n_0}{(k_B T_e)^2 (1 + \Delta_0/k_B T_e)} \exp\left(-\frac{\varepsilon_{\mathbf{k}_{\parallel}}^s - \Delta_0}{k_B T_e}\right),$$

and $n_0 = (m_s^*/2\pi\hbar^2)E_F^s = (\Delta_0/2\pi\hbar^2 v_F^2)E_F^s = (k_B T^*/\pi\hbar^2 v_F^2)E_F^s \sim \alpha_0(L_A - L_0)$. We use $\gamma = +1$ and $q_0 = \Gamma_0/\hbar v_F$ as a cutoff for $q_{\parallel} \rightarrow 0$. $\mathbf{k}_{\parallel}^{\pm}$ stands for $\mathbf{k}_{\parallel} \pm \mathbf{q}_{\parallel}$ and $D = C_0 + \ln(T_e/T^*) - 1/2 \ln 2 (T_e/T^*)^2$. Here, pair scattering of bulk electrons will lead to reduction of total conductivity.

Important conclusions can be drawn from these theoretical results. Firstly, for a weak magnetic field B , the longitudinal conductivity becomes independent of B , although the Hall conductivity depends on B (see Eqns. 2 and 3). Furthermore, Eqn. 5 for the energy relaxation time indicates that both pair scattering and screening effects from EEI do not depend on B . This is a strong argument in favor analyzing EEI by applying a weak magnetic field, in order to separate quantum corrections due to WAL from $\delta\sigma$ (see Eqn. 1 and Fig. 4(b)).

Secondly, the experimentally found strong increase of EEI with the sample thickness (see Fig. 4(a)) can be directly derived from the theory. Eqn. 4 gives the dominant EEI-induced change in surface longitudinal conductivity at low B fields and reveals its thickness dependence. On the one hand, we know that $\delta\sigma \propto \sigma_0^s \sim (L_A - L_0)$. On the other hand, we find that the ratio $\tau_0^s/\tau_{\text{pair}}^s \propto n_0 \sim (L_A - L_0)$. Overall, $\delta\sigma \propto (L_A - L_0)^2$ which for $(L_A - L_0)/L_0 \ll 1$ leads to $\delta\sigma \propto L_A$. This linear relationship describes our experimental findings remarkably well (see Fig. 4(a)). Finally, bulk electrons can also screen impurity scattering of surface electrons, but it becomes insignificant due to the large separation between the surface layer and the center of film.

The fact that $n = 2$ indicates that 2 independent 2D channels are involved and stands in contrast to the results of WAL measurements (see Ref.¹⁸ and Fig. 4(d)). This discrepancy between WAL and EEI has been reported in Cu-doped BiSe single layers²⁷ and attributed to a 2D bulk state. For SbTe single layers²⁸, it was speculated that one coupled state of top and bottom TSS dominates WAL, but that they contribute independently to EEI. It is not clear how coupling could be mediated in our bilayer samples, since the depletion layer at the interface separates the SbTe and BiTe layer. Therefore, it is more likely that the 2D bulk plays a role in EEI processes in our samples.

Lastly, we determine the WAL contribution from the difference between the saturated and zero field amplitude Δf . We have shown already that EEI is independent of the magnetic

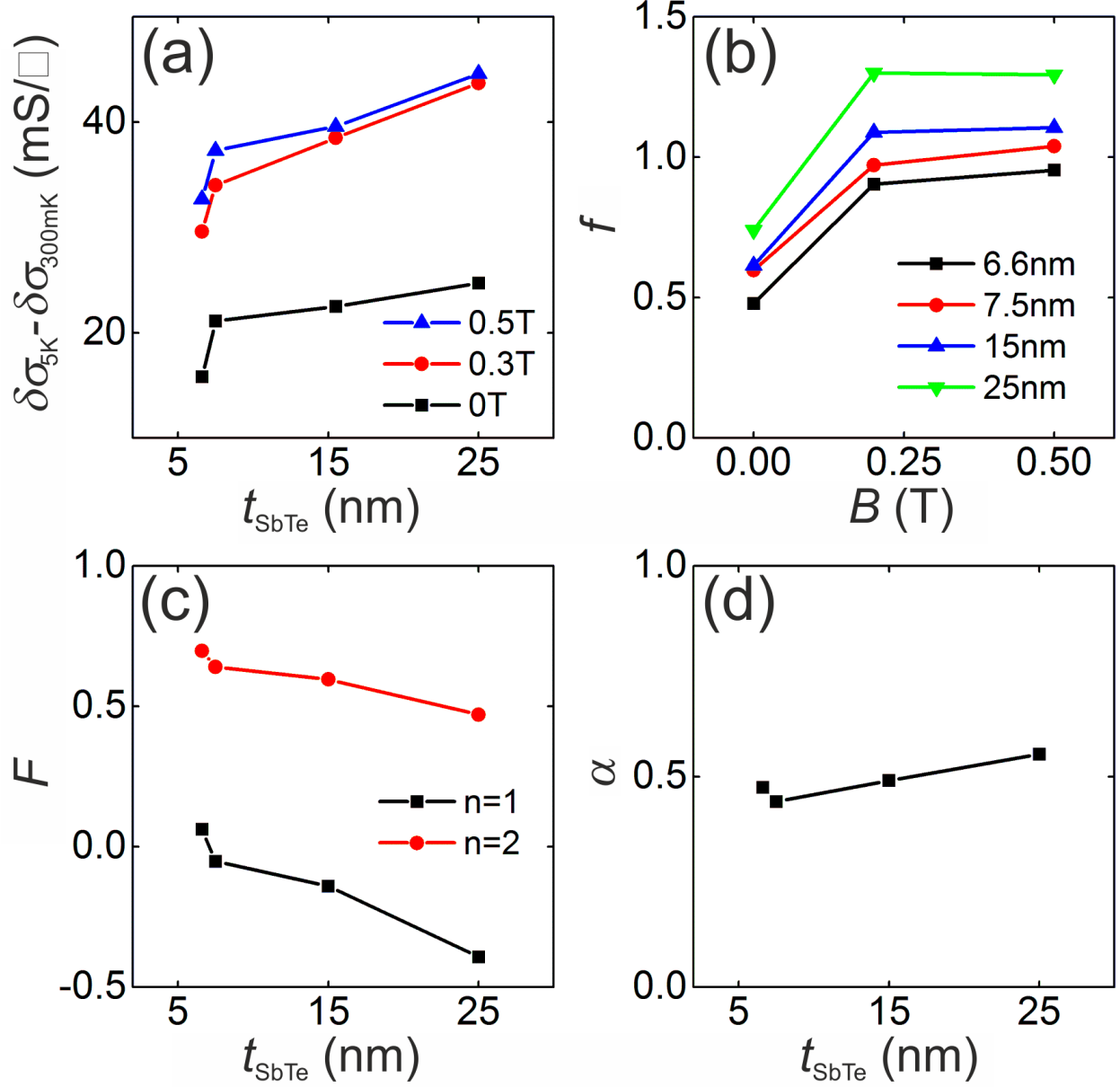


FIG. 4. (a) Difference of conductivity correction $\delta\sigma$ between 5 K and base temperature as a function of the Sb_2Te_3 -thickness. (b) Change of the slope f with an external, perpendicular magnetic field, as shown in Fig. 3. (c) The screening factor F calculated from $f = n(1 - 3/4 * F)$, assuming the number of 2D states n is 1 (black squares) or 2 (red circles). The screening is negative for $n = 1$ and between 0 and 1 for $n = 2$, supporting the presence of more than one 2D channel. (d) Number of 2D channels α from WAL, obtained as described in the text. A value of 0.5 corresponds to one 2D channel.

field, and thus the change of the slope of the $\delta\sigma$ with and without applied field can be attributed to WAL alone. The number of 2D states can be calculated using $\Delta f = p \times \alpha$ with $p = 1$, which characterizes the temperature dependence of the coherence length (see Ref.¹⁸). We obtain $\alpha \approx 0.5$, i.e. that only one TSS is present at all thicknesses^{18,33,34} (see Fig. 4(d)). Since a TSS on the top surface has been confirmed in ARPES experiments¹⁷, we conclude that the TSS at the bottom must be disrupted.

In summary, topological p - n junctions exhibit a rich set of transport characteristics related to their topological surface states. At low temperature, WAL and EEI compete in reducing the conductivity. The fact that EEI are unaffected by an external magnetic field was taken advantage of to determine the number of 2D channels. While exactly one was found from WAL, at least two are contributing to EEI. The growing presence of bulk states does not lead to stronger screening. On the contrary, conductivity corrections due to EEI are getting stronger with increase thickness. This effect could be understood withing a semiclassical Boltzmann theory.

ACKNOWLEDGMENTS

D.B., D.R. and V.N. acknowledge funding from the Leverhulme Trust, UK, D.B., R.M., D.R., and V.N. acknowledge funding from EPSRC (UK). D.H. would like to thank the support from the Air Force Office of Scientific Research (AFOSR). G.M., M.L., J.K. and D.G. acknowledge financial support from the DFG-funded priority programme SPP1666.

* d.backes@lboro.ac.uk

† vn237@cam.ac.uk

- ¹ M. Z. Hasan and C. L. Kane, *Rev. Mod. Phys.* **82**, 3045 (2010).
- ² F. D. M. Haldane, *Phys. Rev. Lett.* **61**, 2015 (1988).
- ³ R. Yu, W. Zhang, H. J. Zhang, S. C. Zhang, X. Dai, and Z. Fang, *Science* **329**, 61 (2010).
- ⁴ C. Z. Chang, J. Zhang, X. Feng, J. Shen, and Z. Zhang, *Science* **340**, 167 (2013).
- ⁵ J. G. Analytis, R. D. McDonald, S. C. Riggs, J. H. Chu, G. S. Boebinger, and I. R. Fisher, *Nature Phys.* **6**, 960 (2010).
- ⁶ J. G. Checkelsky, Y. S. Hor, R. J. Cava, and N. P. Ong, *Phys. Rev. Lett.* **106**, 196801 (2011).
- ⁷ A. A. Taskin, S. Sasaki, K. Segawa, and Y. Ando, *Phys. Rev. Lett.* **109**, 066803 (2012).
- ⁸ Y. L. Chen, J. G. Analytis, J. H. Chu, Z. K. Liu, S. K. Mo, X. L. Qi, H. J. Zhang, D. H. Lu, X. Dai, Z. Fang, S. C. Zhang, I. R. Fisher, Z. Hussain, and Z. X. Shen, *Science* **325**, 178 (2009).
- ⁹ D. Kong, Y. Chen, J. J. Cha, Q. Zhang, J. G. Analytis, K. Lai, Z. Liu, S. S. Hong, K. J. Koski, S. K. Mo, Z. Hussain, I. R. Fisher, Z. X. Shen, and Y. Cui, *Nat. Nanotechnol.* **6**, 705 (2011).
- ¹⁰ J. Zhang, C. Z. Chang, Z. Zhang, J. Wen, X. Feng, K. Li, M. Liu, K. He, L. Wang, X. Chen, Q. K. Xue, X. Ma, and Y. Wang, *Nature Commun.* **2**, 574 (2011).
- ¹¹ C. Weyrich, M. Droegeler, J. Kampmeier, M. Eschbach, G. Mussler, T. Merzenich, T. Stoica, I. E. Batov, J. Schubert, L. Plucinski, B. Beschoten, C. M. Schneider and C. Stampfer, D. Grützmacher, and T. Schaepers, *J. Phys.: Condens. Matter* **28**, 495501 (2016).
- ¹² J. Chen, H. J. Qin, F. Yang, J. Liu, T. Guan, F. M. Qu, G. H. Zhang, J. R. Shi, X. C. Xie, C. L. Yang, K. H. Wu, Y. Q. Li, and L. Lu, *Phys. Rev. Lett.* **105**, 176602 (2010).
- ¹³ J. Chen, X. Y. He, K. H. Wu, Z. Q. Ji, L. Lu, J. R. Shi, J. H. Smet, and Y. Q. Li, *Phys. Rev. B* **83**, 241304 (2011).
- ¹⁴ H. Steinberg, J. B. Laloë, V. Fatemi, J. S. Moodera, and P. Jarillo-Herrero, *Phys. Rev. B* **84**, 233101 (2011).
- ¹⁵ Y. Jiang, Y. Wang, M. Chen, Z. Li, C. Song, K. He, L. Wang, X. Chen, X. Ma, and Q. K. Xue, *Phys. Rev. Lett.* **108**, 016401 (2012).
- ¹⁶ Z. Zhang, X. Feng, M. Guo, Y. Ou, J. Zhang, K. Li, L. Wang, X. Chen, Q. Xue, X. Ma, K. He, and Y. Wang, *Phys. Status Solidi RRL* **7**, 142 (2013).

- ¹⁷ M. Eschbach, E. Mlynczak, J. Kellner, J. Kampmeier, M. Lanius, E. Neumann, C. Weyrich, M. Gehlmann, P. Gospodaric, S. Doring, G. Mussler, N. Demarina, M. Luysberg, G. Bihlmayer, T. Schapers, L. Plucinski, S. Blugel, M. Morgenstern, C. M. Schneider, and D. Grützmacher, *Nature Comm.* **6**, 8816 (2015).
- ¹⁸ D. Backes, D. Huang, R. Mansell, M. Lanius, J. Kampmeier, D. Ritchie, G. Mussler, G. Gumbs, D. Grützmacher, and V. Narayan, *Phys. Rev. B* **96**, 125125 (2017).
- ¹⁹ P. A. Lee and T. V. Ramakrishnan, *Rev. Mod. Phys.* **57**, 287 (1985).
- ²⁰ B. L. Altshuler, A. G. Aronov, and D. E. Khmel'nitsky, *J. Phys. C: Sol. St. Phys.* **15**, 7367 (1998).
- ²¹ E. J. König, P. M. Ostrovsky, I. V. Protopopov, I. V. Gornyi, I. S. Burmistrov, and A. D. Mirlin, *Phys. Rev. B* **88**, 035106 (2013).
- ²² H. Z. Lu and S. Q. Shen, *Phys. Rev. Lett.* **112**, 146601 (2014).
- ²³ J. G. Checkelsky, Y. S. Hor, and M. H. Liu, D. X. Qu, and R. J. Cava, and N. P. Ong, *Phys. Rev. Lett.* **103**, 246601 (2009).
- ²⁴ T.-A. Nguyen, D. Backes, A. Singh, R. Mansell, C. Barnes, D. A. Ritchie, G. Mussler, M. Lanius, D. Grützmacher, and V. Narayan, *Sci. Rep.* **6**, 27716 (2016).
- ²⁵ V. Narayan, T.-A. Nguyen, R. Mansell, D. Ritchie, and G. Mussler, *Phys. Status Solidi RRL* **10**, 253 (2016).
- ²⁶ J. Wang, A. M. DaSilva, C. Z. Chang, K. He, J. K. Jain, N. Samarth, X. C. Ma, Q. K. Xue, and M. H. W. Chan, *Phys. Rev. B* **83**, 245438 (2011).
- ²⁷ Y. Takagaki, A. Giussani, K. Perumal, R. Calarco, and K. J. Friedland, *Phys. Rev. B* **86**, 125137 (2012).
- ²⁸ Y. Takagaki, B. Jenichen, U. Jahn, M. Ramsteiner, and K. J. Friedland, *Phys. Rev. B* **85**, 115314 (2012).
- ²⁹ S. P. Chiu and J. J. Lin, *Phys. Rev. B* **87**, 035122 (2013).
- ³⁰ A. Roy, S. Guchhait, S. Sonde, R. Dey, T. Pramanik, A. Rai, H. C. P. Movva, L. Colombo, and S. K. Banerjee, *Appl. Phys. Lett.* **102**, 163118 (2013).
- ³¹ Y. Takagaki, U. Jahn, A. Giussani, and R. Calarco, *J. Phys. Condens. Matter* **26**, 95802 (2014).
- ³² R. Dey, T. Pramanik, A. Roy, A. Rai, S. Guchhait, S. Sonde, H. C. P. Movva, L. Colombo, L. F. Register, and S. K. Banerjee, *Appl. Phys. Lett.* **104**, 223111 (2014).
- ³³ Y. Jing, S. Huang, K. Zhang, J. Wu, Y. Guo, H. Peng, Z. Liu, and H. Q. Xu, *Nanoscale* **8**, 1879

(2016).

- ³⁴ T. Trivedi, S. Sonde, H. C. P. Movva, and S. K. Banerjee, *J. Appl. Phys.* **119**, 055706 (2016).
- ³⁵ A. Y. Kuntsevich, A. A. Gabdullin, V. A. Prudkogliad, Y. G. Selivanov, E. G. Chizhevskii, and V. M. Pudalov, *Phys. Rev. B* **94**, 235401 (2016).
- ³⁶ P. Sahu, J. Y. Chen, J. C. Myers, and J. P. Wang, *Appl. Phys. Lett.* **112**, 122402 (2018).
- ³⁷ W. J. Wang, K. H. Gao, and Z. Q. Li, *Sci. Rep.* **6**, 25291 (2016).
- ³⁸ see Supplementary Material

Appendix A: Bulk Boltzmann Moment Equation

For an n -doped semiconductor bulk material, we will start with the standard semiclassical Boltzmann transport equation for electrons within a conduction band $\varepsilon_c(\mathbf{k})$ of a bulk. For this case, the electron distribution function $f_c(\mathbf{r}, \mathbf{k}; t)$ satisfies

$$\begin{aligned} & \frac{\partial f_c(\mathbf{r}, \mathbf{k}; t)}{\partial t} + \left\langle \frac{d\mathbf{R}_0(t)}{dt} \right\rangle_{\text{av}} \cdot \nabla_{\mathbf{r}} f_c(\mathbf{r}, \mathbf{k}; t) \\ & + \left\langle \frac{d\mathbf{K}_0(t)}{dt} \right\rangle_{\text{av}} \cdot \nabla_{\mathbf{k}} f_c(\mathbf{r}, \mathbf{k}; t) = \left. \frac{\partial f_c(\mathbf{r}, \mathbf{k}; t)}{\partial t} \right|_{\text{coll}} , \end{aligned} \quad (\text{A1})$$

where \mathbf{r} is a three-dimensional position vector, \mathbf{k} is a three-dimensional wave vector, and the term on the right-hand side of this equation corresponds to the collision contribution of electrons with other electrons, impurities, and phonons. Moreover, for conduction-band electrons, we can define, in a semiclassical way¹, their group velocity through $\mathbf{v}_c(\mathbf{k}) = \nabla_{\mathbf{k}} \varepsilon_c(\mathbf{k}) / \hbar \equiv \langle d\mathbf{R}_0(t) / dt \rangle_{\text{av}}$, where $\mathbf{R}_0(t)$ is the center-of-mass position vector. Furthermore, we introduce the semiclassical Newton-like force equation¹ for the wave vector of miniband electrons, yielding

$$\hbar \left\langle \frac{d\mathbf{K}_0(t)}{dt} \right\rangle_{\text{av}} = \mathbf{F}_c(\mathbf{k}, t) = -e [\mathbf{E}(t) + \mathbf{v}_c(\mathbf{k}) \times \mathbf{B}(t)] , \quad (\text{A2})$$

where $\mathbf{K}_0(t)$ is the center-of-mass wave vector, $\mathbf{E}(t)$ and $\mathbf{B}(t)$ are the external electric and magnetic fields, respectively, and $\mathbf{F}_c(\mathbf{k}, t)$ is the electromagnetic force acting on an electron in the \mathbf{k} state.

Based on Eq. (A1), the zeroth-order Boltzmann moment equation can be obtained by summing over all the \mathbf{k} states on both sides of this equation. This gives rise to the electron number conservation equation, i.e.,

$$\frac{\partial \rho_c}{\partial t} + \nabla_{\mathbf{r}} \cdot \mathbf{J}_c = 0 , \quad (\text{A3})$$

where the electron number volume density $\rho_c(\mathbf{r}, t)$ and particle-number current density $\mathbf{J}_c(\mathbf{r}, t)$ (per area) are defined by

$$\rho_c(\mathbf{r}, t) \equiv \frac{2}{\mathcal{V}} \sum_{\mathbf{k}} f_c(\mathbf{r}, \mathbf{k}; t) , \quad (\text{A4})$$

$$\mathbf{J}_c(\mathbf{r}, t) \equiv \frac{2}{\mathcal{V}} \sum_{\mathbf{k}} \mathbf{v}_c(\mathbf{k}) f_c(\mathbf{r}, \mathbf{k}; t), \quad (\text{A5})$$

and \mathcal{V} is the sample volume.

For the first-order Boltzmann moment equation, we have to employ the so-called Fermi kinetics. Therefore, we first introduce the *relaxation-time approximation* for the electron collision, given by

$$\left. \frac{\partial f_c(\mathbf{r}, \mathbf{k}; t)}{\partial t} \right|_{coll} = - \frac{f_c(\mathbf{r}, \mathbf{k}; t) - f_0[\varepsilon_c(\mathbf{k}), T; u_c]}{\tau_c(k)}, \quad (\text{A6})$$

where $f_0[\varepsilon_c(\mathbf{k}), T; u_c] = \{\exp[\varepsilon_c(\mathbf{k}) - u_c]/k_B T] + 1\}^{-1}$ is the Fermi function for electrons in thermal-equilibrium states, T is the lattice temperature, u_c is the chemical potential of electrons in the system, and $\tau_c(k)$ is the energy-relaxation time for electrons in the \mathbf{k} state. The detailed calculation of $\tau_c(k)$ has been presented in Appendix D. The chemical potential u_c of the system is determined self-consistently by

$$2 \sum_{\mathbf{k}} f_0[\varepsilon_c(\mathbf{k}), T; u_c] = \int d^3\mathbf{r} \rho_c(\mathbf{r}, t) \equiv \frac{2}{\mathcal{V}} \sum_{\mathbf{k}} \int d^3\mathbf{r} f_c(\mathbf{r}, \mathbf{k}; t) = N_e, \quad (\text{A7})$$

where N_e represents the total number of electrons in the system. Finally, by applying this relaxation-time approximation to the standard Boltzmann transport equation in Eq. (A1), we obtain

$$\begin{aligned} f_c(\mathbf{r}, \mathbf{k}; t) + \tau_e(T, u_c) \frac{\partial f_c(\mathbf{r}, \mathbf{k}; t)}{\partial t} &\approx f_0[\varepsilon_c(\mathbf{k}), T; u_c] \\ - \frac{\tau_e(T, u_c)}{\hbar} \mathbf{F}_c(\mathbf{k}, t) \cdot \nabla_{\mathbf{k}} f_0[\varepsilon_c(\mathbf{k}), T; u_c] - \tau_e(T, u_c) \nabla_{\mathbf{r}} \cdot \{ \mathbf{v}_c(\mathbf{k}) f_0[\varepsilon_c(\mathbf{k}), T; u_c] \} \\ &= f_0[\varepsilon_c(\mathbf{k}), T; u_c] - \frac{\tau_e(T, u_c)}{\hbar} \mathbf{F}_c(\mathbf{k}, t) \cdot \nabla_{\mathbf{k}} f_0[\varepsilon_c(\mathbf{k}), T; u_c], \end{aligned} \quad (\text{A8})$$

where we have used the fact that T is spatially uniform throughout the system and equals the lattice temperature, and the statistically-averaged energy-relaxation time $\tau_e(T, u_c)$ is defined by

$$\frac{1}{\tau_e(T, u_c)} = \frac{2}{N_e} \sum_{\mathbf{k}} \frac{f_0[\varepsilon_c(\mathbf{k}), T; u_c]}{\tau_c(k)}. \quad (\text{A9})$$

By introducing another inverse momentum-relaxation time tensor $\overleftrightarrow{\tau}_p^{-1}$ and using Eq. (A2), we can further write the *force-balance equation* for a macroscopic drift velocity $\mathbf{v}_d(t)$, which yields

$$\begin{aligned} \frac{d\mathbf{v}_d(t)}{dt} &= -\overleftrightarrow{\tau}_p^{-1} \cdot \mathbf{v}_d(t) + \overleftrightarrow{\mathcal{M}}^{-1} \cdot \mathbf{F}_e(t) \\ &= -\overleftrightarrow{\tau}_p^{-1} \cdot \mathbf{v}_d(t) - e\overleftrightarrow{\mathcal{M}}^{-1} \cdot [\mathbf{E}(t) + \mathbf{v}_d(t) \times \mathbf{B}(t)] = 0, \end{aligned} \quad (\text{A10})$$

where $\mathbf{F}_e(t) = -e[\mathbf{E}(t) + \mathbf{v}_d(t) \times \mathbf{B}(t)]$ is the macroscopic electromagnetic force, and the statistically-averaged inverse effective-mass tensor $\overleftrightarrow{\mathcal{M}}^{-1}$ for conduction-band electrons is given by

$$\mathcal{M}_{ij}^{-1}(T, u_c) = \frac{2}{N_e} \sum_{\mathbf{k}} \left[\frac{1}{\hbar^2} \frac{\partial^2 \varepsilon_c(\mathbf{k})}{\partial k_i \partial k_j} \right] f_0[\varepsilon_c(\mathbf{k}), T; u_c], \quad (\text{A11})$$

and $i, j = x, y, z$. The detailed calculations for the inverse momentum-relaxation time tensor $\overleftrightarrow{\tau}_p^{-1}$ in our system can be found in Appendix E. Moreover, the internal Coulomb force between a pair of electrons will not contribute to this force-balance equation. The solution of Eq. (A10) can be formally expressed as

$$\mathbf{v}_d(t) = \overleftrightarrow{\boldsymbol{\mu}}[\mathbf{B}(t)] \cdot \mathbf{E}(t), \quad (\text{A12})$$

where $\overleftrightarrow{\boldsymbol{\mu}}[\mathbf{B}(t)]$ is the so-called mobility tensor for conduction-band electrons, which also depends on $\overleftrightarrow{\tau}_p^{-1}$ and $\overleftrightarrow{\mathcal{M}}^{-1}$ in addition to $\mathbf{B}(t)$. The details for calculating the mobility tensor $\overleftrightarrow{\boldsymbol{\mu}}[\mathbf{B}(t)]$ are presented in Appendix F. Using Eqs. (A10) and (A12), we can rewrite $\mathbf{F}_e(t) = \left(\overleftrightarrow{\mathcal{M}} \otimes \overleftrightarrow{\tau}_p^{-1} \right) \cdot [\overleftrightarrow{\boldsymbol{\mu}}[\mathbf{B}(t)] \cdot \mathbf{E}(t)]$, where $\overleftrightarrow{\mathcal{M}}$ represents the inverse of $\overleftrightarrow{\mathcal{M}}^{-1}$.

In a similar way, multiplying both sides of Eq. (A8) by $\mathbf{v}_c(\mathbf{k})$ and summing over all the \mathbf{k} states afterwards, we get

$$\begin{aligned} \mathbf{J}_c(t) + \tau_e(T, u_c) \frac{\partial \mathbf{J}_c(t)}{\partial t} &= -\tau_e(T, u_c) \frac{2}{\mathcal{V}} \sum_{\mathbf{k}} \mathbf{v}_c(\mathbf{k}) [\mathbf{F}_e(t) \cdot \mathbf{v}_c(\mathbf{k})] \frac{\partial f_0[\varepsilon_c(\mathbf{k}), T; u_c]}{\partial \varepsilon_c} \\ &= -e\tau_e(T, u_c) \frac{2}{\mathcal{V}} \sum_{\mathbf{k}} \mathbf{v}_c(\mathbf{k}) \left\{ \left(\overleftrightarrow{\mathcal{M}} \otimes \overleftrightarrow{\tau}_p^{-1} \right) \cdot [\overleftrightarrow{\boldsymbol{\mu}}[\mathbf{B}(t)] \cdot \mathbf{E}(t)] \right\} \cdot \mathbf{v}_c(\mathbf{k}) \left[-\frac{\partial f_0[\varepsilon_c(\mathbf{k}), T; u_c]}{\partial \varepsilon_c} \right]. \end{aligned} \quad (\text{A13})$$

From Eq. (A13) we know the particle-number current density \mathbf{J}_c is independent of \mathbf{r} . Consequently, from Eq. (A3) we find that the number volume density ρ_c becomes a constant ρ_0 , determined by

$$\rho_0 = \frac{2}{\mathcal{V}} \sum_{\mathbf{k}} f_0[\varepsilon_c(\mathbf{k}), T; u_c], \quad (\text{A14})$$

which determines the chemical potential u_c of the system for fixed T . If the external fields are static ones, i.e., \mathbf{E}_0 and \mathbf{B}_0 , we get the charge current density \mathbf{J}_0 from Eq. (A13)

$$\mathbf{J}_0 = -e^2 \tau_e \left(\frac{2}{\mathcal{V}} \right) \sum_{\mathbf{k}} \mathbf{v}_c(\mathbf{k}) \left\{ \left(\overset{\leftrightarrow}{\mathcal{M}} \otimes \overset{\leftrightarrow}{\tau}_p^{-1} \right) \cdot [\overset{\leftrightarrow}{\boldsymbol{\mu}}[\mathbf{B}_0] \cdot \mathbf{E}_0] \right\} \cdot \mathbf{v}_c(\mathbf{k}) \left[-\frac{\partial f_0[\varepsilon_c(\mathbf{k}), T; u_c]}{\partial \varepsilon_c} \right]. \quad (\text{A15})$$

In this case, the elements of the conductivity tensor $\overset{\leftrightarrow}{\sigma}(\mathbf{B}_0)$ can be obtained through $\sigma_{ij}(\mathbf{B}_0) = \mathbf{J}_0 \cdot \hat{\mathbf{e}}_i / (\mathbf{E}_0 \cdot \hat{\mathbf{e}}_j)$, where $i, j = x, y, z$ and $\hat{\mathbf{e}}_x, \hat{\mathbf{e}}_y, \hat{\mathbf{e}}_z$ are three unit vectors in a position space. From Eq. (A15), we know that the conductivity tensor depends not only on the mobility tensor, but also on how electrons are distributed within an anisotropic conduction band.

As a special case, we consider an isotropic parabolic band structure given by $\varepsilon_c(\mathbf{k}) = \hbar^2 k^2 / 2m^*$, we find from Eq. (A11) that $\mathcal{M}_{ij}^{-1} = (1/m^*) \delta_{ij}$ and $\mathcal{M}_{ij} = m^* \delta_{ij}$, as well as $(\overset{\leftrightarrow}{\tau}_p^{-1})_{ij} = (1/\tau_p) \delta_{ij}$. In this case, from Eq. (F15) we obtain the mobility tensor as

$$\overset{\leftrightarrow}{\boldsymbol{\mu}}[\mathbf{B}(t)] = -\frac{\mu_0}{1 + \mu_0^2 B^2} \begin{bmatrix} 1 + \mu_0^2 B_x^2 & -\mu_0 B_z + \mu_0^2 B_x B_y & \mu_0 B_y + \mu_0^2 B_x B_z \\ \mu_0 B_z + \mu_0^2 B_y B_x & 1 + \mu_0^2 B_y^2 & -\mu_0 B_x + \mu_0^2 B_y B_z \\ -\mu_0 B_y + \mu_0^2 B_z B_x & \mu_0 B_x + \mu_0^2 B_z B_y & 1 + \mu_0^2 B_z^2 \end{bmatrix}, \quad (\text{A16})$$

where $\mu_0 = e\tau_p/m^*$, $\mathbf{B} = \{B_x, B_y, B_z\}$, and $B^2 = B_x^2 + B_y^2 + B_z^2$. If we further assume $\mathbf{B} = 0$, Eq. (A16) simply leads to $\mu_{ij} = -\mu_0 \delta_{ij}$. In this case, from Eq. (A15) we get the well-known result $\mathbf{J}_0 = (\rho_0 e^2 \tau_e / m^*) \mathbf{E}_0$, which implies $\sigma_{ij} = (\rho_0 e^2 \tau_e / m^*) \delta_{ij}$. For a p -doped semiconductor bulk material, similar equations can be derived for $f_v(\mathbf{r}, \mathbf{k}; t)$, $\rho_v(\mathbf{r}, t)$ and $\mathbf{J}_v(t)$ with replacements of $\varepsilon_c(\mathbf{k})$, $\mathbf{r}_c(t)$, $\mathbf{F}_e(t)$, $\tau_c(\mathbf{k})$, u_c , $-e$ by $\varepsilon_v(\mathbf{k})$, $\mathbf{r}_v(t)$, $\mathbf{F}_h(t)$, $\tau_v(\mathbf{k})$, u_v , $+e$, respectively.

Appendix B: Surface Boltzmann Moment Equation

For a semiconductor sheet, we will also start with the standard semiclassical Boltzmann transport equation for electrons within conduction subbands $\varepsilon_n(\mathbf{k}_{\parallel})$ of a sheet, where $n = 1, 2$ for two spin-resolved conduction subbands within the bulk semiconductor bandgap. For this case, the electron distribution function $f_n(\mathbf{r}_{\parallel}, \mathbf{k}_{\parallel}; t)$ satisfies

$$\begin{aligned} & \frac{\partial f_n(\mathbf{r}_{\parallel}, \mathbf{k}_{\parallel}; t)}{\partial t} + \left\langle \frac{d\mathbf{R}_{\parallel}(t)}{dt} \right\rangle_{\text{av}} \cdot \nabla_{\mathbf{r}_{\parallel}} f_n(\mathbf{r}_{\parallel}, \mathbf{k}_{\parallel}; t) \\ & + \left\langle \frac{d\mathbf{K}_{\parallel}(t)}{dt} \right\rangle_{\text{av}} \cdot \nabla_{\mathbf{k}_{\parallel}} f_n(\mathbf{r}_{\parallel}, \mathbf{k}_{\parallel}; t) = \left. \frac{\partial f_n(\mathbf{r}_{\parallel}, \mathbf{k}_{\parallel}; t)}{\partial t} \right|_{\text{coll}} , \end{aligned} \quad (\text{B1})$$

where \mathbf{r}_{\parallel} is a two-dimensional position vector on the bulk surface, \mathbf{k}_{\parallel} is a two-dimensional wave vector within the surface plane, and the term at the right-hand side of this equation corresponds to the collision contribution of electrons with other electrons, impurities, and phonons. Moreover, for conduction-subband electrons, we can define, in a semiclassical way, their group velocity through $\mathbf{v}_n(\mathbf{k}_{\parallel}) = \nabla_{\mathbf{k}_{\parallel}} \varepsilon_n(\mathbf{k}_{\parallel}) / \hbar \equiv \langle d\mathbf{R}_{\parallel}(t)/dt \rangle_{\text{av}}$. Furthermore, we introduce the semiclassical Newton-like force equation for the wave vector of miniband electrons, yielding

$$\hbar \left\langle \frac{d\mathbf{K}_{\parallel}(t)}{dt} \right\rangle_{\text{av}} \equiv \mathbf{F}_n(\mathbf{k}_{\parallel}, t) = -e [\mathbf{E}(t) + \mathbf{v}_n(\mathbf{k}_{\parallel}) \times \mathbf{B}(t)] , \quad (\text{B2})$$

where $\mathbf{E}(t)$ and $\mathbf{B}(t)$ are the external electric and magnetic fields, respectively, and $\mathbf{F}_n(\mathbf{k}_{\parallel}, t)$ is the electromagnetic force acted on an electron in the \mathbf{k}_{\parallel} state of the n th subband.

Based on Eq.(B1), the zeroth-order Boltzmann moment equation can be obtained by summing over all the \mathbf{k}_{\parallel} states and all the subbands on both sides of this equation. This gives rise to the electron number conservation equation, i.e.,

$$\frac{\partial n_s}{\partial t} + \nabla_{\mathbf{r}_{\parallel}} \cdot \mathbf{j}_s = 0 , \quad (\text{B3})$$

where the surface density of electron number $n_s(\mathbf{r}_{\parallel}, t)$ and surface particle-number current density $\mathbf{j}_s(\mathbf{r}_{\parallel}, t)$ (per length) are defined by

$$n_s(\mathbf{r}_{\parallel}, t) \equiv \frac{1}{\mathcal{A}} \sum_{n, \mathbf{k}_{\parallel}} f_n(\mathbf{r}_{\parallel}, \mathbf{k}_{\parallel}; t) , \quad (\text{B4})$$

$$\mathbf{j}_s(\mathbf{r}_{\parallel}, t) \equiv \frac{1}{\mathcal{A}} \sum_{n, \mathbf{k}_{\parallel}} \mathbf{v}_n(\mathbf{k}_{\parallel}) f_n(\mathbf{r}_{\parallel}, \mathbf{k}_{\parallel}; t), \quad (\text{B5})$$

\mathcal{A} is the surface area.

For the first-order Boltzmann moment equation, we again have to employ the so-called Fermi kinetics. Therefore, we first introduce the relaxation-time approximation for the electron collision, given by

$$\left. \frac{\partial f_n(\mathbf{r}_{\parallel}, \mathbf{k}_{\parallel}; t)}{\partial t} \right|_{coll} = - \frac{f_n(\mathbf{r}_{\parallel}, \mathbf{k}_{\parallel}; t) - f_0[\varepsilon_n(\mathbf{k}_{\parallel}), T; u_s]}{\tau_n(k_{\parallel})}, \quad (\text{B6})$$

where $f_0[\varepsilon_n(\mathbf{k}_{\parallel}), T; u_s] = \{\exp[\varepsilon_n(\mathbf{k}_{\parallel}) - u_s/k_B T] + 1\}^{-1}$ is the Fermi function for electrons in thermal-equilibrium states, T is the lattice temperature, u_s is the chemical potential of surface electrons and $\tau_n(k_{\parallel})$ is the energy-relaxation time for electrons in the \mathbf{k}_{\parallel} state of the n th subband. The surface chemical potential u_s is determined self-consistently by

$$\sum_{n, \mathbf{k}_{\parallel}} f_0[\varepsilon_n(\mathbf{k}_{\parallel}), T; u_s] = \int d^2 \mathbf{r}_{\parallel} n_s(\mathbf{r}_{\parallel}, t) \equiv \frac{1}{\mathcal{A}} \sum_{n, \mathbf{k}_{\parallel}} \int d^2 \mathbf{r}_{\parallel} f_n(\mathbf{r}_{\parallel}, \mathbf{k}_{\parallel}; t) = N_s, \quad (\text{B7})$$

where $N_s = n_0 \mathcal{A}$ represents the total number of surface electrons for each spin and n_0 is the areal density for surface electrons. Finally, by applying this relaxation-time approximation to the standard Boltzmann transport equation in Eq. (B1), we obtain

$$\begin{aligned} f_n(\mathbf{r}_{\parallel}, \mathbf{k}_{\parallel}; t) + \tau_s(T, u_s) \frac{\partial f_n(\mathbf{r}_{\parallel}, \mathbf{k}_{\parallel}; t)}{\partial t} &\approx f_0[\varepsilon_n(\mathbf{k}_{\parallel}), T; u_s] \\ - \frac{\tau_s(T, u_s)}{\hbar} \mathbf{F}_n(\mathbf{k}_{\parallel}, t) \cdot \nabla_{\mathbf{k}_{\parallel}} f_0[\varepsilon_n(\mathbf{k}_{\parallel}), T; u_s] - \tau_s(T, u_s) \nabla_{\mathbf{r}_{\parallel}} \cdot \{ \mathbf{v}_n(\mathbf{k}_{\parallel}) f_0[\varepsilon_n(\mathbf{k}_{\parallel}), T; u_s] \} \\ &= f_0[\varepsilon_n(\mathbf{k}_{\parallel}), T; u_s] - \frac{\tau_s(T, u_s)}{\hbar} \mathbf{F}_n(\mathbf{k}_{\parallel}, t) \cdot \nabla_{\mathbf{k}_{\parallel}} f_0[\varepsilon_n(\mathbf{k}_{\parallel}), T; u_s], \end{aligned} \quad (\text{B8})$$

where we have used the fact that T is uniform throughout the system and equals the lattice temperature, and the statistically-averaged surface energy-relaxation time $\tau_s(T, u_s)$ is defined by

$$\frac{1}{\tau_s(T, u_s)} = \frac{1}{N_s} \sum_{n, \mathbf{k}_{\parallel}} \frac{f_0[\varepsilon_n(\mathbf{k}_{\parallel}), T; u_s]}{\tau_n(k_{\parallel})}. \quad (\text{B9})$$

By introducing another inverse surface momentum-relaxation time tensor $\overleftrightarrow{\tau}_{sp}^{-1}$ and using Eq.(B2), we can further write the force-balance equation for the macroscopic surface drift velocity $\mathbf{v}_s(t)$, which yields

$$\begin{aligned} \frac{d\mathbf{v}_s(t)}{dt} &= -\overleftrightarrow{\tau}_{sp}^{-1} \cdot \mathbf{v}_s(t) + \overleftrightarrow{\mathcal{M}}_s^{-1} \cdot \mathbf{F}_s(t) \\ &= -\overleftrightarrow{\tau}_{sp}^{-1} \cdot \mathbf{v}_s(t) - e\overleftrightarrow{\mathcal{M}}_s^{-1} \cdot [\mathbf{E}(t) + \mathbf{v}_s(t) \times \mathbf{B}(t)] = 0, \end{aligned} \quad (\text{B10})$$

where the macroscopic surface electromagnetic force is $\mathbf{F}_s(t) = -e[\mathbf{E}(t) + \mathbf{v}_s(t) \times \mathbf{B}(t)]$, and the statistically-averaged inverse effective-mass tensor for surface electrons is given by

$$(\mathcal{M}_s^{-1})_{ij} = \frac{1}{N_s} \sum_{n, \mathbf{k}_{\parallel}} \left[\frac{1}{\hbar^2} \frac{\partial^2 \varepsilon_n(\mathbf{k}_{\parallel})}{\partial k_{i\parallel} \partial k_{j\parallel}} \right] f_0[\varepsilon_n(\mathbf{k}_{\parallel}), T; u_s], \quad (\text{B11})$$

and $i, j = x, y$. The solution of Eq. (B10) can be formally written as

$$\mathbf{v}_s(t) = \overleftrightarrow{\boldsymbol{\mu}}_s[\mathbf{B}(t)] \cdot \mathbf{E}(t), \quad (\text{B12})$$

where $\overleftrightarrow{\boldsymbol{\mu}}_s[\mathbf{B}(t)]$ is the so-called mobility tensor for surface electrons, which also depends on $\overleftrightarrow{\tau}_{sp}^{-1}$ and $\overleftrightarrow{\mathcal{M}}_s^{-1}$ in addition to $\mathbf{B}(t)$. Using Eqs.(B10) and (B12), we can rewrite $\mathbf{F}_s(t) = \left(\overleftrightarrow{\mathcal{M}}_s \otimes \overleftrightarrow{\tau}_p^{-1} \right) \cdot [\overleftrightarrow{\boldsymbol{\mu}}_s[\mathbf{B}(t)] \cdot \mathbf{E}(t)]$, where $\overleftrightarrow{\mathcal{M}}_s$ represents the inverse of $\overleftrightarrow{\mathcal{M}}_s^{-1}$.

In a similar way, multiplying both sides of Eq. (B8) by $\mathbf{v}_n(\mathbf{k}_{\parallel})$ and summing over all the \mathbf{k}_{\parallel} states and all the subbands afterwards, we get

$$\begin{aligned} \mathbf{j}_s(t) + \tau_s(T, u_s) \frac{\partial \mathbf{j}_s(t)}{\partial t} &= -\tau_s(T, u_s) \frac{1}{\mathcal{A}} \sum_{n, \mathbf{k}_{\parallel}} \mathbf{v}_n(\mathbf{k}_{\parallel}) [\mathbf{F}_s(t) \cdot \mathbf{v}_n(\mathbf{k}_{\parallel})] \frac{\partial f_0[\varepsilon_n(\mathbf{k}_{\parallel}), T; u_s]}{\partial \varepsilon_n} \\ &= e\tau_s(T, u_s) \frac{1}{\mathcal{A}} \sum_{n, \mathbf{k}_{\parallel}} \mathbf{v}_n(\mathbf{k}_{\parallel}) \left\{ \left(\overleftrightarrow{\mathcal{M}}_s \otimes \overleftrightarrow{\tau}_{sp}^{-1} \right) \cdot [\overleftrightarrow{\boldsymbol{\mu}}_s[\mathbf{B}(t)] \cdot \mathbf{E}(t)] \right\} \cdot \mathbf{v}_n(\mathbf{k}_{\parallel}) \left[-\frac{\partial f_0[\varepsilon_n(\mathbf{k}_{\parallel}), T; u_s]}{\partial \varepsilon_n} \right]. \end{aligned} \quad (\text{B13})$$

From Eq. (B13) we know the surface particle-number current density \mathbf{j}_s is independent of \mathbf{r}_{\parallel} . As a result, from Eq. (B3) we find the surface number areal density n_s becomes a constant n_0 , determined by

$$n_0 = \frac{1}{\mathcal{A}} \sum_{n, \mathbf{k}_{\parallel}} f_0[\varepsilon_n(\mathbf{k}_{\parallel}), T; u_s], \quad (\text{B14})$$

which determines the surface chemical potential u_s for fixed T . If the external fields are static ones, i.e., \mathbf{E}_0 and \mathbf{B}_0 , we get the surface charge-current density \mathbf{j}_0 from Eq. (B13)

$$\mathbf{j}_0 = e^2 \tau_s \left(\frac{1}{\mathcal{A}} \right) \sum_{n, \mathbf{k}_{\parallel}} \mathbf{v}_n(\mathbf{k}_{\parallel}) \left\{ \left(\overleftrightarrow{\mathcal{M}}_s \otimes \overleftrightarrow{\tau}_{sp}^{-1} \right) \cdot [\overleftrightarrow{\boldsymbol{\mu}}_s[\mathbf{B}_0] \cdot \mathbf{E}_0] \right\} \cdot \mathbf{v}_n(\mathbf{k}_{\parallel}) \left[-\frac{\partial f_0[\varepsilon_n(\mathbf{k}_{\parallel}), T; u_s]}{\partial \varepsilon_c} \right]. \quad (\text{B15})$$

In this case, the elements of the conductivity tensor $\overleftrightarrow{\boldsymbol{\sigma}}(\mathbf{B}_0)$ can be obtained through $\sigma_{ij}(\mathbf{B}_0) = \mathbf{j}_0 \cdot \hat{\mathbf{e}}_i / (\mathbf{E}_0 \cdot \hat{\mathbf{e}}_j)$, where $i, j = x, y$ and $\hat{\mathbf{e}}_x, \hat{\mathbf{e}}_y$ are the unit vectors. From Eq. (B15), we know that the conductivity tensor not only depends on the mobility tensor, but also depends on how electrons are distributed within anisotropic conduction subbands.

Appendix C: Coulomb Effect on Surface Conductivity

From Eqs. (E6) and (E14), we find the total inverse momentum-relaxation-time tensor $\overleftrightarrow{\tau}_{sp}^{-1} = \overleftrightarrow{\tau}_{s,i}^{-1} + \overleftrightarrow{\tau}_{s,ph}^{-1}$ in Eq. (B15) through

$$\overleftrightarrow{\tau}_{s,i}^{-1} = -\frac{2\sigma_i}{n_0 \mathcal{A}} \sum_{\mathbf{q}_{\parallel}} |U_i(q_{\parallel})|^2 \left\{ \frac{\partial \text{Im} [\Pi_s(q_{\parallel}, \omega)]}{\partial \omega} \right\}_{\omega=\Gamma_0} \left\{ \overleftrightarrow{\mathcal{M}}_s^{-1} \otimes [\mathbf{q}_{\parallel} \otimes \mathbf{q}_{\parallel}^T] \right\}, \quad (\text{C1})$$

and

$$\begin{aligned} \overleftrightarrow{\tau}_{s,ph}^{-1} &= -\frac{4}{n_0 \mathcal{A}} \sum_{\mathbf{q}_{\parallel}, \lambda} |C_{q_{\parallel}, \lambda}|^2 \left\{ \frac{\partial \text{Im} [\Pi_s(q_{\parallel}, \omega)]}{\partial \omega} \right\}_{\omega=\omega_{q_{\parallel}, \lambda}} \\ &\times \left[N_0(\omega_{q_{\parallel}, \lambda}, T) - N_0(\omega_{q_{\parallel}, \lambda} + \mathbf{q}_{\parallel} \cdot \mathbf{v}_d, T_e) \right] \left\{ \overleftrightarrow{\mathcal{M}}_s^{-1} \otimes [\mathbf{q}_{\parallel} \otimes \mathbf{q}_{\parallel}^T] \right\} \\ &\quad - \frac{4}{n_0 \mathcal{A}} \sum_{\mathbf{q}_{\parallel}} |C_{q_{\parallel}}|^2 \left\{ \frac{\partial \text{Im} [\Pi_s(q_{\parallel}, \omega)]}{\partial \omega} \right\}_{\omega=\omega_{\text{LO}}} \\ &\times \left[N_0(\omega_{\text{LO}}, T) - N_0(\omega_{\text{LO}} + \mathbf{q}_{\parallel} \cdot \mathbf{v}_d, T_e) \right] \left\{ \overleftrightarrow{\mathcal{M}}_s^{-1} \otimes [\mathbf{q}_{\parallel} \otimes \mathbf{q}_{\parallel}^T] \right\} \end{aligned} \quad (\text{C2})$$

with

$$[\mathbf{q}_{\parallel} \otimes \mathbf{q}_{\parallel}^T] \equiv \begin{bmatrix} q_x^2 & q_x q_y \\ q_y q_x & q_y^2 \end{bmatrix},$$

where Γ_0 is the inverse of particle lifetime due to vertex correction, σ_i is the areal density of impurities, $\omega_{q_{\parallel}\lambda}$ and ω_{LO} are the frequencies of acoustic and longitudinal-optical phonons, $N_0(\omega, T) = [\exp(\hbar\omega/k_B T) - 1]^{-1}$ is the Bose function for thermal-equilibrium phonons, and T_e is the hot-electron temperature due to inelastic phonon scatterings. Here, we assume that only the lowest subband of surface electrons is occupied, and the imaginary part of the *screened* polarization function, $\text{Im} [\Pi_s(q_{\parallel}, \omega)]$, is given by

$$\text{Im} [\Pi_s(q_{\parallel}, \omega)] = \frac{\text{Im} [\Pi_s^{(0)}(q_{\parallel}, \omega)]}{\left\{ 1 - v_s(q_{\parallel}) \text{Re} [\Pi_s^{(0)}(q_{\parallel}, \omega)] \right\}^2 + \left\{ v_s(q_{\parallel}) \text{Im} [\Pi_s^{(0)}(q_{\parallel}, \omega)] \right\}^2}, \quad (\text{C3})$$

where the denominator represents the screening effect, $v_s(q_{\parallel}) = (e^2/2\epsilon_0\epsilon_b q_{\parallel}) \exp(-q_{\parallel}\delta_s)$ is the two-dimensional Fourier transform of a bare Coulomb potential, ϵ_b is the dielectric constant of the host material and δ_s is the thickness of the surface layer. Moreover, the *bare* polarization function $\Pi_s^{(0)}(q_{\parallel}, \omega)$ in Eq. (C3) is calculated within the random-phase approximation as

$$\Pi_s^{(0)}(q_{\parallel}, \omega) = \frac{2}{\mathcal{A}} \sum_{\gamma, \gamma' = \pm 1} \sum_{\mathbf{k}_{\parallel}} \mathcal{F}_{\gamma, \gamma'}(\mathbf{k}_{\parallel}, \mathbf{q}_{\parallel}) \frac{f_{\gamma, \mathbf{k}_{\parallel}}^s - f_{\gamma', \mathbf{k}_{\parallel} + \mathbf{q}_{\parallel}}^s}{\hbar\omega + i0^+ - \varepsilon_{\gamma', \mathbf{k}_{\parallel} + \mathbf{q}_{\parallel}}^s + \varepsilon_{\gamma, \mathbf{k}_{\parallel}}^s}, \quad (\text{C4})$$

where the overlapping factor for zero-bandgap is given by

$$\mathcal{F}_{\gamma, \gamma'}(\mathbf{k}_{\parallel}, \mathbf{q}_{\parallel}) = \frac{1}{2} \left[1 + \gamma\gamma' \frac{\mathbf{k}_{\parallel} \cdot (\mathbf{k}_{\parallel} + \mathbf{q}_{\parallel})}{|\mathbf{k}_{\parallel}| |\mathbf{k}_{\parallel} + \mathbf{q}_{\parallel}|} \right],$$

$\varepsilon_{\gamma, \mathbf{k}_{\parallel}}^s = \gamma \varepsilon_{\mathbf{k}_{\parallel}}^s$ and $f_{\gamma, \mathbf{k}_{\parallel}}^s = f_0[\varepsilon_{\gamma, \mathbf{k}_{\parallel}}^s, T_e; u_s] = \left\{ 1 + \exp \left[(\gamma \varepsilon_{\mathbf{k}_{\parallel}}^s - u_s)/k_B T_e \right] \right\}^{-1}$ is the Fermi-Dirac function for thermal-equilibrium surface electrons at an elevated temperature T_e .

Let us first consider the case with a zero bandgap, i.e., $\Delta_0 = 0$. For $T_e = 0$ and in the long-wavelength limit ($q_{\parallel} \rightarrow 0$), we obtain² from Eq. (C4)

$$\text{Re} [\Pi_s^{(0)}(q_{\parallel}, \omega)] = \frac{q_{\parallel}^2}{4\pi\hbar\omega} \left[\frac{4E_F^s}{\hbar\omega} + \ln \left| \frac{2E_F^s - \hbar\omega}{2E_F^s + \hbar\omega} \right| \right], \quad (\text{C5})$$

$$\text{Im} [\Pi_s^{(0)}(q_{\parallel}, \omega)] = -\frac{q_{\parallel}^2}{4\hbar\omega} \Theta(\hbar\omega - 2E_F^s), \quad (\text{C6})$$

where $\Theta(x)$ is a unit-step function, $E_F^s = \hbar v_F k_F^s$ and $k_F^s = \sqrt{4\pi n_0}$. On the other hand, in the high-temperature $k_B T_e \gg E_F^s$, $\hbar\omega$ and long-wavelength $q_{\parallel} \rightarrow 0$ limits, we arrive at²

$$\text{Re} [\Pi_s^{(0)}(q_{\parallel}, \omega)] = \frac{2 \ln 2}{\pi} \left(\frac{q_{\parallel}^2}{\hbar^2 \omega^2} \right) k_B T_e \left[1 + \frac{(E_F^s)^4}{128 (\ln 2)^3 (k_B T_e)^4} \right], \quad (\text{C7})$$

$$\text{Im} [\Pi_s^{(0)}(q_{\parallel}, \omega)] = -\frac{q_{\parallel}^2}{16 k_B T_e} \left[1 - \frac{\hbar^2 \omega^2}{48 (k_B T_e)^2} \right]. \quad (\text{C8})$$

For $T_e \neq 0$ but $k_B T_e \ll E_F^s$, $\hbar \omega$, the zero-temperature results in Eqs. (C5) and (C6) can be formally generalized to²

$$\text{Re} [\Pi_s^{(0)}(q_{\parallel}, \omega)] = \frac{q_{\parallel}^2}{4\pi \hbar \omega} \left[\frac{4u_s(T_e)}{\hbar \omega} + \ln \left| \frac{2u_s(T_e) - \hbar \omega}{2u_s(T_e) + \hbar \omega} \right| \right], \quad (\text{C9})$$

$$\text{Im} [\Pi_s^{(0)}(q_{\parallel}, \omega)] = -\frac{q_{\parallel}^2}{8\hbar \omega} \left[1 + \tanh \left(\frac{\hbar \omega - 2u_s(T_e)}{4k_B T_e} \right) \right] \quad (\text{C10})$$

with a chemical potential at finite temperatures

$$u_s(T_e) \approx E_F^s \left[1 - \frac{\pi^2}{6} \left(\frac{k_B T_e}{E_F^s} \right)^2 \right].$$

If we further consider a *gaped and undoped* subband for surface electrons with an energy gap Δ_0 and $E_F^s \rightarrow 0$, then we acquire the generalized overlapping factor

$$\mathcal{F}_{\gamma, \gamma'}(\mathbf{k}_{\parallel}, \mathbf{q}_{\parallel}) = \frac{1}{2} \left[1 + \gamma \gamma' \frac{(\hbar v_F)^2 \mathbf{k}_{\parallel} \cdot (\mathbf{k}_{\parallel} + \mathbf{q}_{\parallel}) + \Delta_0^2}{\sqrt{\hbar^2 v_F^2 |\mathbf{k}_{\parallel}|^2 + \Delta_0^2} \sqrt{\hbar^2 v_F^2 |\mathbf{k}_{\parallel} + \mathbf{q}_{\parallel}|^2 + \Delta_0^2}} \right].$$

Moreover, Eq. (C4) under the condition of $k_B T_e \gg \Delta_0$, $\hbar \omega$ turns into²

$$\text{Re} [\Pi_s^{(0)}(q_{\parallel}, \omega)] = \frac{4k_B T_e q_{\parallel}^2}{\pi \hbar^2 \omega^2} \left\{ 2 \ln 2 - \left(\frac{\Delta_0}{k_B T_e} \right)^2 \left[C_0 - \ln \left(\frac{\Delta_0}{2k_B T_e} \right) \right] \right\}, \quad (\text{C11})$$

$$\text{Im} [\Pi_s^{(0)}(q_{\parallel}, \omega)] = -\frac{q_{\parallel}^2}{16 k_B T_e} \left(1 - \frac{\Delta_0}{\hbar \omega} \right), \quad (\text{C12})$$

where $C_0 \approx 0.79$ is a constant.

Firstly, let us consider only the impurity scattering at low temperatures. We know from Eq. (C1) that $\hat{\boldsymbol{\tau}}_{sp}^{-1}$ becomes diagonal and its identical diagonal element $1/\tau_{sp}$ is given by

$$\frac{1}{\tau_{sp}} = -\frac{\sigma_i}{2\pi n_0 m^*} \left(\frac{Z^* e^2}{2\epsilon_0 \epsilon_b} \right)^2 \int_0^{1/\delta_s} dq_{\parallel} q_{\parallel} \left\{ \frac{\partial \text{Im} [\Pi_s(q_{\parallel}, \omega)]}{\partial \omega} \right\}_{\omega=\Gamma_0}. \quad (\text{C13})$$

By making use of the results in Eqs. (C11) and (C12), Eq. (C13) for impurity scattering leads to

$$\frac{1}{\tau_{sp}} \approx \frac{v_F^2}{128\pi\hbar\Gamma_0^2\delta_s^2 k_B T^*} \left(\frac{\sigma_i}{n_0} \right) \left(\frac{Z^* e^2}{2\epsilon_0 \epsilon_b \delta_s} \right)^2 \left(\frac{T^*}{T_e} \right) \times \left\{ 1 - \frac{128}{5\pi\hbar\Gamma_0} \left(\frac{e^2}{2\epsilon_0 \epsilon_b \delta_s} \right) \left(1 - \frac{3k_B T^*}{\hbar\Gamma_0} \right) \left(\frac{T^*}{T_e} \right) \left[C_0 + \ln \left(\frac{T_e}{T^*} \right) - \frac{\ln 2}{2} \left(\frac{T_e}{T^*} \right)^2 \right] \right\}, \quad (\text{C14})$$

which satisfies $1/\tau_{e,h} \propto 1/n_0 \sim (L_A - L_0)^{-1}$, where we have used $1/m_s^* = v_F^2/\Delta_0$ and defined $T^* = \Delta_0/2k_B$.

The results for phonon scattering can be obtained in a similar way. Furthermore, we find from Eq. (B15) that

$$\mathbf{j}_0 = \left(\frac{e^2 v_F^2 \tau_s}{\Delta_0 \tau_{sp}} \right) \frac{1}{\mathcal{A}} \sum_{\mathbf{k}_{\parallel}} \mathbf{v}_{\mathbf{k}_{\parallel}}^s \left\{ \hat{\mathcal{I}}_0 \cdot [\hat{\boldsymbol{\mu}}_s[\mathbf{B}_0] \cdot \mathbf{E}_0] \right\} \cdot \mathbf{v}_{\mathbf{k}_{\parallel}}^s \left[-\frac{\partial f_0[\varepsilon_{\mathbf{k}_{\parallel}}^s, T_e; u_s]}{\partial \varepsilon_{\mathbf{k}_{\parallel}}^s} \right], \quad (\text{C15})$$

where $\mathbf{v}_{\mathbf{k}_{\parallel}}^s = \hbar v_F^2 \mathbf{k}_{\parallel} / \Delta_0 = \hbar v_F^2 \mathbf{k}_{\parallel} / 2k_B T^*$ is the group velocity of surface electrons and $\tau_s(T_e, u_s)$ is the statistically averaged energy-relaxation time $\tau_s(\mathbf{k}_{\parallel})$.

Secondly, including the *screened* pair scattering of surface electrons, we get $1/\tau_{\text{pair}}^s(T, u_s)$ from Eqs. (D1)-(D3), as well as from Eqs. (C11) and (C12), yielding

$$\begin{aligned} \frac{1}{\tau_{\text{pair}}^s(T_e, u_s)} &= \frac{1}{n_0 \mathcal{A}} \sum_{\mathbf{k}_{\parallel}} \frac{f_{\mathbf{k}_{\parallel}}^s}{\tau_{\text{pair}}^s(\mathbf{k}_{\parallel})} \approx \frac{1}{16\pi^4 \hbar n_0} \left(\frac{e^2}{2\epsilon_0 \epsilon_b} \right)^2 \\ &\times \int_{q_0}^{1/\delta_s} \frac{dq_{\parallel}}{q_{\parallel}} \left\{ 1 - q_{\parallel} \left(\frac{e^2}{2\epsilon_0 \epsilon_b} \right) \frac{32k_B T^*}{\pi \hbar^2 \Gamma_0^2} \left(\frac{T^*}{T_e} \right) \left[C_0 + \ln \left(\frac{T_e}{T^*} \right) - \frac{\ln 2}{2} \left(\frac{T_e}{T^*} \right)^2 \right] \right\} \\ &\times \int d^2 \mathbf{k}_{\parallel} f_{\mathbf{k}_{\parallel}}^s \int d^2 \mathbf{k}'_{\parallel} \left[f_{\mathbf{k}'_{\parallel}}^s (1 - f_{\mathbf{k}_{\parallel} - \mathbf{q}_{\parallel}}^s) (1 - f_{\mathbf{k}'_{\parallel} + \mathbf{q}_{\parallel}}^s) + f_{\mathbf{k}_{\parallel} - \mathbf{q}_{\parallel}}^s f_{\mathbf{k}'_{\parallel} + \mathbf{q}_{\parallel}}^s (1 - f_{\mathbf{k}'_{\parallel}}^s) \right] \\ &\times \frac{\Gamma_0 / \pi}{(\varepsilon_{\mathbf{k}_{\parallel}}^s + \varepsilon_{\mathbf{k}'_{\parallel}}^s - \varepsilon_{\mathbf{k}_{\parallel} - \mathbf{q}_{\parallel}}^s - \varepsilon_{\mathbf{k}'_{\parallel} + \mathbf{q}_{\parallel}}^s)^2 + \Gamma_0^2}, \end{aligned} \quad (\text{C16})$$

where

$$f_{\mathbf{k}_{\parallel}}^s \approx \frac{2\pi \hbar^2 v_F^2 n_0}{(k_B T_e)^2 (1 + \Delta_0 / k_B T_e)} \exp \left(-\frac{\varepsilon_{\mathbf{k}_{\parallel}}^s - \Delta_0}{k_B T_e} \right), \quad (\text{C17})$$

$n_0 = (m_s^*/2\pi\hbar^2)E_F^s = (\Delta_0/2\pi\hbar^2v_F^2)E_F^s = (k_B T^*/\pi\hbar^2v_F^2)E_F^s \sim \alpha_0(L_A - L_0)$ with L_A as the acceptor-layer thickness, $\gamma \equiv 1$ is taken and $q_0 = \Gamma_0/\hbar v_F$ is a cutoff for $q_{\parallel} \rightarrow 0$. Here, pair scattering of bulk electrons will lead to reduction of total conductivity. Furthermore, $1/\tau_{\text{pair}}^s(T_e, u_s)$ has its density dependence of both $\sim n_0$ and $\sim n_0^2$. In principle, bulk electrons can also screen impurity scattering of surface electrons, but it becomes insignificant due to large separation between the surface layer and the center of the film.

Finally, by using Eq. (G5) the total conductivity is calculated as

$$\begin{aligned} \overleftrightarrow{\sigma}_{\text{tot}}(\mathbf{B}) &= e \overleftrightarrow{\mu}_v^{\parallel}(\mathbf{B}) N_A A_h \left[(L_A - W_p) + \int_0^{W_p} dz \exp\left(-\frac{\beta e \bar{\mu}_h N_A}{2\epsilon_0 \epsilon_r D_h} z^2\right) \right] - e \overleftrightarrow{\mu}_c^{\parallel}(\mathbf{B}) N_D A_e \\ &\times \left[(L_D - W_n) + \int_0^{W_n} dz \exp\left(-\frac{\beta e \bar{\mu}_e N_D}{2\epsilon_0 \epsilon_r D_e} z^2\right) \right] + e \overleftrightarrow{\mu}_s^{\pm}(\mathbf{B}) \left(\frac{\alpha_0 \Delta_0}{2\pi\hbar^2 v_F^2} \right) (L_A - L_0) A_s, \end{aligned} \quad (\text{C18})$$

where $A_s = \tau_s/\tau_{sp}$ and $A_{e,h} = \tau_{e,h}/\tau_{p(e,h)}$. Here, the surface mobility is given by

$$\overleftrightarrow{\mu}_s(\mathbf{B}) = \frac{\mu_1}{1 + \mu_1^2 B^2} \begin{bmatrix} 1 & \mu_1 B \\ -\mu_1 B & 1 \end{bmatrix}, \quad (\text{C19})$$

and $\mu_1 = e\tau_{sp}v_F^2/\Delta_0 = e\tau_{sp}v_F^2/2k_B T^*$. For weak magnetic field, we have $\mu_1 B \ll 1$, $\mu_{xx} = \mu_{yy} = \mu_1$ and $\mu_{xy} = -\mu_{yx} = \mu_1^2 B$. As $\mathbf{B} \rightarrow 0$, we find from Eqs. (C18) and (C19) that the change of the total conductivity due to the screened pair scattering of surface electrons is given by

$$\begin{aligned} \delta\sigma_{\text{tot}}(T_e, u_s) &\equiv \sigma_{\text{tot}}(T_e, u_s) - \sigma_{\text{tot}}^{(0)}(T_e, u_s) \\ &= -\mu_0^s \left(\frac{\alpha_0 \Delta_0}{2\pi\hbar^2 v_F^2} \right) (L_A - L_0) \left[\frac{\tau_0^s(T_e, u_s)}{\tau_0^s(T_e, u_s) + \tau_{\text{pair}}^s(T_e, u_s)} \right] \approx -\sigma_0^s \left[\frac{\tau_0^s(T_e, u_s)}{\tau_{\text{pair}}^s(T_e, u_s)} \right], \end{aligned} \quad (\text{C20})$$

where $\mu_0^s = e\tau_0^s v_F^2/\Delta_0 = e\tau_0^s v_F^2/2k_B T^*$, σ_0^s and τ_0^s are the mobility, conductivity and energy-relaxation time, respectively, of surface electrons in the absence of electron-electron interaction (EEI).

Therefore, from Eq. (C20) we know $\delta\sigma_{\text{tot}}(T_e, u_s) \propto \sigma_0^s \sim (L_A - L_0)$. Meanwhile, we also find the ratio $\tau_0^s/\tau_{\text{pair}}^s \propto n_0 \sim (L_A - L_0)$, as can be seen from Eqs. (C16) and (D2). Although the screening due to electron-electron interaction can weaken the impurity scattering and increases the mobility, the conductivity is not affected by the momentum-relaxation time τ_{sp} of surface electrons. Even for two-dimensional electron gases in a quantum well, where they

acquire a static dielectric function³ $\epsilon_s(q_{\parallel}) \equiv \epsilon(q_{\parallel}, \omega = 0) = 1 + q_s/q_{\parallel}$ with a Thomas-Fermi screening length $1/q_s$, the screened impurity scattering can also increase their conductivity.

Appendix D: Energy-Relaxation Time

By using the detailed-balance condition, the energy-relaxation time $\tau_c(k)$ initially introduced in Eq. (A6) can be calculated according to⁴

$$\frac{1}{\tau_c(k)} = \mathcal{W}_{\text{in}}(k) + \mathcal{W}_{\text{out}}(k) , \quad (\text{D1})$$

where the scattering-in rate for electrons in the final \mathbf{k} -state is

$$\begin{aligned} \mathcal{W}_{\text{in}}(k) = & n_i \frac{2\pi}{\hbar\mathcal{V}} \sum_{\mathbf{q}} |U_i(q)|^2 [f_{\mathbf{k}-\mathbf{q}} \delta(\varepsilon_{\mathbf{k}} - \varepsilon_{\mathbf{k}-\mathbf{q}}) + f_{\mathbf{k}+\mathbf{q}} \delta(\varepsilon_{\mathbf{k}} - \varepsilon_{\mathbf{k}+\mathbf{q}})] \\ & + \frac{2\pi}{\hbar\mathcal{V}} \sum_{\mathbf{q},\lambda} |C_{q\lambda}|^2 \{f_{\mathbf{k}-\mathbf{q}} N_0(\omega_{q\lambda}) \delta(\varepsilon_{\mathbf{k}} - \varepsilon_{\mathbf{k}-\mathbf{q}} - \hbar\omega_{q\lambda}) \\ & \quad + f_{\mathbf{k}+\mathbf{q}} [N_0(\omega_{q\lambda}) + 1] \delta(\varepsilon_{\mathbf{k}} - \varepsilon_{\mathbf{k}+\mathbf{q}} + \hbar\omega_{q\lambda})\} \\ & + \frac{2\pi}{\hbar\mathcal{V}} \sum_{\mathbf{q}} |C_q|^2 \{f_{\mathbf{k}-\mathbf{q}} N_0(\omega_{\text{LO}}) \delta(\varepsilon_{\mathbf{k}} - \varepsilon_{\mathbf{k}-\mathbf{q}} - \hbar\omega_{\text{LO}}) \\ & \quad + f_{\mathbf{k}+\mathbf{q}} [N_0(\omega_{\text{LO}}) + 1] \delta(\varepsilon_{\mathbf{k}} - \varepsilon_{\mathbf{k}+\mathbf{q}} + \hbar\omega_{\text{LO}})\} \\ & + \frac{2\pi}{\hbar\mathcal{V}^2} \sum_{\mathbf{k}',\mathbf{q}} |V_c(q)|^2 (1 - f_{\mathbf{k}'}) f_{\mathbf{k}-\mathbf{q}} f_{\mathbf{k}'+\mathbf{q}} \delta(\varepsilon_{\mathbf{k}} + \varepsilon_{\mathbf{k}'} - \varepsilon_{\mathbf{k}-\mathbf{q}} - \varepsilon_{\mathbf{k}'+\mathbf{q}}) , \end{aligned} \quad (\text{D2})$$

and the scattering-out rate for electrons in the initial \mathbf{k} -state is

$$\begin{aligned} \mathcal{W}_{\text{out}}(k) = & n_i \frac{2\pi}{\hbar\mathcal{V}} \sum_{\mathbf{q}} |U_i(q)|^2 [(1 - f_{\mathbf{k}+\mathbf{q}}) \delta(\varepsilon_{\mathbf{k}+\mathbf{q}} - \varepsilon_{\mathbf{k}}) + (1 - f_{\mathbf{k}-\mathbf{q}}) \delta(\varepsilon_{\mathbf{k}-\mathbf{q}} - \varepsilon_{\mathbf{k}})] \\ & + \frac{2\pi}{\hbar\mathcal{V}} \sum_{\mathbf{q},\lambda} |C_{q\lambda}|^2 \{(1 - f_{\mathbf{k}+\mathbf{q}}) N_0(\omega_{q\lambda}) \delta(\varepsilon_{\mathbf{k}+\mathbf{q}} - \varepsilon_{\mathbf{k}} - \hbar\omega_{q\lambda}) \\ & \quad + (1 - f_{\mathbf{k}-\mathbf{q}}) [N_0(\omega_{q\lambda}) + 1] \delta(\varepsilon_{\mathbf{k}-\mathbf{q}} - \varepsilon_{\mathbf{k}} + \hbar\omega_{q\lambda})\} \\ & + \frac{2\pi}{\hbar\mathcal{V}} \sum_{\mathbf{q}} |C_q|^2 \{(1 - f_{\mathbf{k}+\mathbf{q}}) N_0(\omega_{\text{LO}}) \delta(\varepsilon_{\mathbf{k}+\mathbf{q}} - \varepsilon_{\mathbf{k}} - \hbar\omega_{\text{LO}}) \\ & \quad + (1 - f_{\mathbf{k}-\mathbf{q}}) [N_0(\omega_{\text{LO}}) + 1] \delta(\varepsilon_{\mathbf{k}-\mathbf{q}} - \varepsilon_{\mathbf{k}} + \hbar\omega_{\text{LO}})\} \\ & + \frac{2\pi}{\hbar\mathcal{V}^2} \sum_{\mathbf{k}',\mathbf{q}} |V_c(q)|^2 f_{\mathbf{k}'} (1 - f_{\mathbf{k}-\mathbf{q}}) (1 - f_{\mathbf{k}'+\mathbf{q}}) \delta(\varepsilon_{\mathbf{k}-\mathbf{q}} + \varepsilon_{\mathbf{k}'+\mathbf{q}} - \varepsilon_{\mathbf{k}} - \varepsilon_{\mathbf{k}'}) . \end{aligned} \quad (\text{D3})$$

Here, n_i is the volume density of ionized impurities. For simplicity, we have introduced the notations, $f_{\mathbf{k}} \equiv f_0[\varepsilon_c(\mathbf{k}), T; u_c]$, $\varepsilon_{\mathbf{k}} \equiv \varepsilon_c(\mathbf{k})$, and $N_0(x) = [\exp(\hbar x/k_B T) - 1]^{-1}$ is the

Bose function for thermal-equilibrium phonons, and $\hbar\omega_{q\lambda}$ ($\hbar\omega_{\text{LO}}$) is the energy of acoustic (longitudinal-optical) phonons, respectively.

For the electron-impurity scattering, $N_i = n_i\mathcal{V}$ represents the total number of impurities in the system, and

$$|U_i(q)| = \frac{Z^*e^2}{\epsilon_0\epsilon_b(q^2 + Q_c^2)}, \quad (\text{D4})$$

where Z^* is the charge number of fully-ionized impurity atoms.

For the scattering of electrons with acoustic phonons, we have

$$|C_{q\ell}|^2 = \frac{\hbar}{2\rho_i\omega_{q\ell}} \left[D_0^2 q^2 + \frac{9}{32} (eh_{14})^2 \right] \frac{q^2}{(q^2 + Q_c^2)}, \quad (\text{D5})$$

$$|C_{qt}|^2 = \frac{\hbar}{2\rho_i\omega_{qt}} \frac{13}{64} (eh_{14})^2 \frac{q^2}{(q^2 + Q_c^2)}, \quad (\text{D6})$$

where $\lambda = \ell, t$ represents the longitudinal (ℓ) and transverse (t) acoustic phonons, respectively, ρ_i is the ion mass density, D_0 is the deformation potential, and h_{14} is the piezoelectric constant.

For the scattering of electrons with longitudinal-optical phonons, on the other hand, we find

$$|C_q|^2 = \frac{\hbar\omega_{\text{LO}}}{2} \left(\frac{1}{\epsilon_\infty} - \frac{1}{\epsilon_s} \right) \frac{e^2}{\epsilon_0(q^2 + Q_c^2)}, \quad (\text{D7})$$

where ϵ_s and ϵ_∞ are the static and high-frequency dielectric constants of the host semiconductors.

Finally, for the scattering between two electrons, we require

$$V_c(q) = \frac{e^2}{\epsilon_0\epsilon_b(q^2 + Q_c^2)}. \quad (\text{D8})$$

For the surface case, the wave vector \mathbf{k} should be replaced by \mathbf{k}_\parallel , and the Coulomb potential $1/[(q^2 + Q_c^2)]$ should be replaced by $\exp(-q_\parallel\delta_s)/2[(q_\parallel + q_c)]$, where δ_s represents the thickness of the surface layer.

Appendix E: Inverse Momentum-Relaxation-Time Tensor

The inverse momentum-relaxation-time tensor $\hat{\tau}_p^{-1}$ initially introduced in Eq. (A10) comes from the statistically-averaged frictional forces $\mathbf{F}_x = \mathbf{F}_x^i + \mathbf{F}_x^{ph}$ due to scattering of electrons with impurities (i) and phonons (ph).

For electrons moving with a drift velocity \mathbf{v}_d , the frictional force \mathbf{F}_x^i from the impurity scattering is calculated as⁵

$$\mathbf{F}_x^i = -n_i \frac{2\pi}{\hbar\mathcal{V}} \sum_{\mathbf{k}, \mathbf{q}} \hbar\mathbf{q} (\hbar\mathbf{q} \cdot \mathbf{v}_d) |U_i(q)|^2 \left(-\frac{\partial f_{\mathbf{k}}}{\partial \varepsilon_{\mathbf{k}}} \right) \delta(\varepsilon_{\mathbf{k}+\mathbf{q}} - \varepsilon_{\mathbf{k}}), \quad (\text{E1})$$

and we have $\hat{\tau}_i^{-1} \cdot \mathbf{v}_d = -(2/N_e) \hat{\mathcal{M}}^{-1} \cdot \mathbf{F}_x^i$, where

$$\hat{\tau}_i^{-1} = \frac{4\pi\hbar n_i}{\rho_0 \mathcal{V}^2} \sum_{\mathbf{k}, \mathbf{q}} |U_i(q)|^2 \left(-\frac{\partial f_{\mathbf{k}}}{\partial \varepsilon_{\mathbf{k}}} \right) \delta(\varepsilon_{\mathbf{k}+\mathbf{q}} - \varepsilon_{\mathbf{k}}) \left\{ \hat{\mathcal{M}}^{-1} \otimes [\mathbf{q} \otimes \mathbf{q}^T] \right\}, \quad (\text{E2})$$

ρ_0 and n_i are the volume densities of electrons and impurities, and

$$[\mathbf{q} \otimes \mathbf{q}^T] \equiv \begin{bmatrix} q_x^2 & q_x q_y & q_x q_z \\ q_y q_x & q_y^2 & q_y q_z \\ q_z q_x & q_z q_y & q_z^2 \end{bmatrix}.$$

Physically, we can rewrite Eq. (E1) as

$$\mathbf{F}_x^i = n_i \sum_{\mathbf{q}} \mathbf{q} |U_i(q)|^2 \text{Im} [\Pi(\mathbf{q}, \mathbf{q} \cdot \mathbf{v}_d)], \quad (\text{E3})$$

where

$$\text{Im} [\Pi(\mathbf{q}, \omega)] = \frac{\text{Im} [\Pi^{(0)}(\mathbf{q}, \omega)]}{\{1 - v_c(q) \text{Re} [\Pi^{(0)}(\mathbf{q}, \omega)]\}^2 + \{v_c(q) \text{Im} [\Pi^{(0)}(\mathbf{q}, \omega)]\}^2}, \quad (\text{E4})$$

and $v_c(q) = e^2/\epsilon_0\epsilon_b q^2$ is the Fourier transform of a bare Coulomb potential. Moreover, the bare polarization function $\Pi^{(0)}(\mathbf{q}, \omega)$ introduced in Eq. (E4) is calculated within the random-phase approximation as

$$\Pi^{(0)}(\mathbf{q}, \omega) = \frac{2}{\mathcal{V}} \sum_{\mathbf{k}} \frac{f_{\mathbf{k}} - f_{\mathbf{k}+\mathbf{q}}}{\hbar\omega + i0^+ - \varepsilon_{\mathbf{k}+\mathbf{q}} + \varepsilon_{\mathbf{k}}}. \quad (\text{E5})$$

Therefore, by using Eq. (E3), the inverse momentum-relaxation-time tensor $\overleftrightarrow{\boldsymbol{\tau}}_i^{-1}$ given by Eq. (E2) can be rewritten into the form

$$\overleftrightarrow{\boldsymbol{\tau}}_i^{-1} = -\frac{2n_i}{\rho_0\mathcal{V}} \sum_{\mathbf{q}} |U_i(q)|^2 \left\{ \frac{\partial \text{Im} [\Pi(\mathbf{q}, \omega)]}{\partial \omega} \right\}_{\omega=\Gamma_0} \left\{ \overleftrightarrow{\mathcal{M}}^{-1} \otimes [\mathbf{q} \otimes \mathbf{q}^T] \right\}, \quad (\text{E6})$$

where Γ_0 is the inverse of particle lifetime.

Similarly, for electrons moving with a drift velocity \mathbf{v}_d , the frictional force \mathbf{F}_x^{ph} from the acoustic and optical phonon scattering is found to be

$$\begin{aligned} \mathbf{F}_x^{ph} &= -\frac{1}{\mathcal{V}} \sum_{\mathbf{k}, \mathbf{q}, \lambda} \hbar \mathbf{q} \left\{ \Theta_{\mathbf{q}\lambda}^{em}(\mathbf{k}) [N_0(\omega_{q\lambda}) + 1] - \Theta_{\mathbf{q}\lambda}^{abs}(\mathbf{k}) N_0(\omega_{q\lambda}) \right\} \\ &\quad - \frac{1}{\mathcal{V}} \sum_{\mathbf{k}, \mathbf{q}} \hbar \mathbf{q} \left\{ \Theta_{\mathbf{q}}^{em}(\mathbf{k}) [N_0(\omega_{LO}) + 1] - \Theta_{\mathbf{q}}^{abs}(\mathbf{k}) N_0(\omega_{LO}) \right\}, \end{aligned} \quad (\text{E7})$$

where the emission and absorption rates for acoustic phonons are

$$\Theta_{\mathbf{q}\lambda}^{em}(\mathbf{k}) = \frac{4\pi}{\hbar} |C_{q\lambda}|^2 (\hbar \mathbf{q} \cdot \mathbf{v}_d) \left(-\frac{\partial f_{\mathbf{k}}}{\partial \varepsilon_{\mathbf{k}}} \right) \delta(\varepsilon_{\mathbf{k}} - \varepsilon_{\mathbf{k}+\mathbf{q}} + \hbar\omega_{q\lambda}), \quad (\text{E8})$$

$$\Theta_{\mathbf{q}\lambda}^{abs}(\mathbf{k}) = -\frac{4\pi}{\hbar} |C_{q\lambda}|^2 (\hbar \mathbf{q} \cdot \mathbf{v}_d) \left(-\frac{\partial f_{\mathbf{k}}}{\partial \varepsilon_{\mathbf{k}}} \right) \delta(\varepsilon_{\mathbf{k}} - \varepsilon_{\mathbf{k}-\mathbf{q}} - \hbar\omega_{q\lambda}). \quad (\text{E9})$$

In a similar way, the emission and absorption rates for longitudinal-optical phonons are calculated as

$$\Theta_{\mathbf{q}}^{em}(\mathbf{k}) = \frac{4\pi}{\hbar} |C_q|^2 (\hbar \mathbf{q} \cdot \mathbf{v}_d) \left(-\frac{\partial f_{\mathbf{k}}}{\partial \varepsilon_{\mathbf{k}}} \right) \delta(\varepsilon_{\mathbf{k}} - \varepsilon_{\mathbf{k}+\mathbf{q}} + \hbar\omega_{LO}), \quad (\text{E10})$$

$$\Theta_{\mathbf{q}}^{abs}(\mathbf{k}) = -\frac{4\pi}{\hbar} |C_q|^2 (\hbar \mathbf{q} \cdot \mathbf{v}_d) \left(-\frac{\partial f_{\mathbf{k}}}{\partial \varepsilon_{\mathbf{k}}} \right) \delta(\varepsilon_{\mathbf{k}} - \varepsilon_{\mathbf{k}-\mathbf{q}} - \hbar\omega_{LO}). \quad (\text{E11})$$

Therefore, from Eq. (E7) we get $\overleftrightarrow{\boldsymbol{\tau}}_{ph}^{-1} \cdot \mathbf{v}_d = -(2/N_e) \overleftrightarrow{\mathcal{M}}^{-1} \cdot \mathbf{F}_x^{ph}$, where

$$\begin{aligned} \overleftrightarrow{\boldsymbol{\tau}}_{ph}^{-1} &= \frac{8\pi\hbar}{\rho_0\mathcal{V}^2} \sum_{\mathbf{k}, \mathbf{q}, \lambda} |C_{q\lambda}|^2 \left(-\frac{\partial f_{\mathbf{k}}}{\partial \varepsilon_{\mathbf{k}}} \right) \left\{ \overleftrightarrow{\mathcal{M}}^{-1} \otimes [\mathbf{q} \otimes \mathbf{q}^T] \right\} \\ &\quad \times \left\{ [N_0(\omega_{q\lambda}) + 1] \delta(\varepsilon_{\mathbf{k}} - \varepsilon_{\mathbf{k}+\mathbf{q}} + \hbar\omega_{q\lambda}) + N_0(\omega_{q\lambda}) \delta(\varepsilon_{\mathbf{k}} - \varepsilon_{\mathbf{k}-\mathbf{q}} - \hbar\omega_{q\lambda}) \right\} \\ &\quad + \frac{8\pi\hbar}{\rho_0\mathcal{V}^2} \sum_{\mathbf{k}, \mathbf{q}} |C_q|^2 \left(-\frac{\partial f_{\mathbf{k}}}{\partial \varepsilon_{\mathbf{k}}} \right) \left\{ \overleftrightarrow{\mathcal{M}}^{-1} \otimes [\mathbf{q} \otimes \mathbf{q}^T] \right\} \\ &\quad \times \left\{ [N_0(\omega_{LO}) + 1] \delta(\varepsilon_{\mathbf{k}} - \varepsilon_{\mathbf{k}+\mathbf{q}} + \hbar\omega_{LO}) + N_0(\omega_{LO}) \delta(\varepsilon_{\mathbf{k}} - \varepsilon_{\mathbf{k}-\mathbf{q}} - \hbar\omega_{LO}) \right\}. \end{aligned} \quad (\text{E12})$$

Again, we can rewrite Eq. (E7) as

$$\begin{aligned} \mathbf{F}_x^{ph} &= 2 \sum_{\mathbf{q}, \lambda} \mathbf{q} |C_{q\lambda}|^2 \text{Im} [\Pi(\mathbf{q}, \omega_{q\lambda} + \mathbf{q} \cdot \mathbf{v}_d)] [N_0(\omega_{q\lambda}, T) - N_0(\omega_{q\lambda} + \mathbf{q} \cdot \mathbf{v}_d, T_e)] \\ &+ 2 \sum_{\mathbf{q}} \mathbf{q} |C_q|^2 \text{Im} [\Pi(\mathbf{q}, \omega_{LO} + \mathbf{q} \cdot \mathbf{v}_d)] [N_0(\omega_{LO}, T) - N_0(\omega_{LO} + \mathbf{q} \cdot \mathbf{v}_d, T_e)] , \end{aligned} \quad (\text{E13})$$

and thus Eq. (E12) becomes

$$\begin{aligned} \overleftrightarrow{\tau}_{ph}^{-1} &= -\frac{4}{\rho_0 \mathcal{V}} \sum_{\mathbf{q}, \lambda} |C_{q\lambda}|^2 \left\{ \frac{\partial \text{Im} [\Pi(\mathbf{q}, \omega)]}{\partial \omega} \right\}_{\omega=\omega_{q\lambda}} \\ &\times [N_0(\omega_{q\lambda}, T) - N_0(\omega_{q\lambda} + \mathbf{q} \cdot \mathbf{v}_d, T_e)] \left\{ \overleftrightarrow{\mathcal{M}}^{-1} \otimes [\mathbf{q} \otimes \mathbf{q}^T] \right\} \\ &- \frac{4}{\rho_0 \mathcal{V}} \sum_{\mathbf{q}} |C_q|^2 \left\{ \frac{\partial \text{Im} [\Pi(\mathbf{q}, \omega)]}{\partial \omega} \right\}_{\omega=\omega_{LO}} \\ &\times [N_0(\omega_{LO}, T) - N_0(\omega_{LO} + \mathbf{q} \cdot \mathbf{v}_d, T_e)] \left\{ \overleftrightarrow{\mathcal{M}}^{-1} \otimes [\mathbf{q} \otimes \mathbf{q}^T] \right\} , \end{aligned} \quad (\text{E14})$$

where T_e is the temperature of hot electrons, determined from the energy-conservation equation⁶:

$$\begin{aligned} (\mathbf{F}_x^i + \mathbf{F}_x^{ph}) \cdot \mathbf{v}_d + 2 \sum_{\mathbf{q}, \lambda} |C_{q\lambda}|^2 \omega_{q\lambda} \text{Im} [\Pi(\mathbf{q}, \omega_{q\lambda} + \mathbf{q} \cdot \mathbf{v}_d)] [N_0(\omega_{q\lambda}, T) - N_0(\omega_{q\lambda} + \mathbf{q} \cdot \mathbf{v}_d, T_e)] \\ + 2 \sum_{\mathbf{q}} |C_q|^2 \omega_{LO} \text{Im} [\Pi(\mathbf{q}, \omega_{LO} + \mathbf{q} \cdot \mathbf{v}_d)] [N_0(\omega_{LO}, T) - N_0(\omega_{LO} + \mathbf{q} \cdot \mathbf{v}_d, T_e)] = 0 . \end{aligned}$$

Finally, the inverse momentum-relaxation-time tensor is simply given by $\overleftrightarrow{\tau}_p^{-1} = \overleftrightarrow{\tau}_i^{-1} + \overleftrightarrow{\tau}_{ph}^{-1}$.

For the surface case, the wave vector \mathbf{q} should be replaced by $\mathbf{q}_{||}$, $q_z = 0$ and both $\overleftrightarrow{\mathcal{M}}_s^{-1}$ and $\overleftrightarrow{\tau}_{sp}^{-1}$ reduce to 2×2 tensors.

Appendix F: Mobility Tensor

From the force-balance equation in Eq. (A10), by using the approximation $\overleftrightarrow{\tau}_p^{-1} \approx (1/\tau_j) \delta_{ij}$ for simplicity, we get the following group of linear equations for $\mathbf{v}_d = \{v_1, v_2, v_3\}$

$$\begin{aligned}
& [1 + q\tau_1 (r_{12}B_3 - r_{13}B_2)] v_1 + q\tau_1 (r_{13}B_1 - r_{11}B_3) v_2 + q\tau_1 (r_{11}B_2 - r_{12}B_1) v_3 \\
& = q\tau_1 (r_{11}E_1 + r_{12}E_2 + r_{13}E_3) , \tag{F1}
\end{aligned}$$

$$\begin{aligned}
& q\tau_2 (r_{22}B_3 - r_{23}B_2) v_1 + [1 + q\tau_2 (r_{23}B_1 - r_{21}B_3)] v_2 + q\tau_2 (r_{21}B_2 - r_{22}B_1) v_3 \\
& = q\tau_2 (r_{21}E_1 + r_{22}E_2 + r_{23}E_3) , \tag{F2}
\end{aligned}$$

$$\begin{aligned}
& q\tau_3 (r_{32}B_3 - r_{33}B_2) v_1 + q\tau_3 (r_{33}B_1 - r_{31}B_3) v_2 + [1 + q\tau_3 (r_{31}B_2 - r_{32}B_1)] v_3 \\
& = q\tau_3 (r_{31}E_1 + r_{32}E_2 + r_{33}E_3) , \tag{F3}
\end{aligned}$$

where we have used the notations $\mathbf{B} = \{B_1, B_2, B_3\}$, $\mathbf{E} = \{E_1, E_2, E_3\}$, $q = -e$ and $\overleftrightarrow{\mathcal{M}}^{-1} = \{r_{ij}\}$. By defining the coefficient matrix $\overleftrightarrow{\mathcal{C}}$ for the above linear equations, i.e.,

$$\overleftrightarrow{\mathcal{C}} = \begin{bmatrix} 1 + q\tau_1(r_{12}B_3 - r_{13}B_2) & q\tau_1(r_{13}B_1 - r_{11}B_3) & q\tau_1(r_{11}B_2 - r_{12}B_1) \\ q\tau_2(r_{22}B_3 - r_{23}B_2) & 1 + q\tau_2(r_{23}B_1 - r_{21}B_3) & q\tau_2(r_{21}B_2 - r_{22}B_1) \\ q\tau_3(r_{32}B_3 - r_{33}B_2) & q\tau_3(r_{33}B_1 - r_{31}B_3) & 1 + q\tau_3(r_{31}B_2 - r_{32}B_1) \end{bmatrix} , \tag{F4}$$

as well as the source vector \mathbf{s} , given by

$$\mathbf{s} = \begin{bmatrix} q\tau_1(r_{11}E_1 + r_{12}E_2 + r_{13}E_3) \\ q\tau_2(r_{21}E_1 + r_{22}E_2 + r_{23}E_3) \\ q\tau_3(r_{31}E_1 + r_{32}E_2 + r_{33}E_3) \end{bmatrix} , \tag{F5}$$

we can reduce the linear equations to a matrix equation $\overleftrightarrow{\mathcal{C}} \cdot \mathbf{v}_d = \mathbf{s}$ with the formal solution $\mathbf{v}_d = \overleftrightarrow{\mathcal{C}}^{-1} \cdot \mathbf{s}$. Explicitly, we find the solution $\mathbf{v}_d = \{v_1, v_2, v_3\}$ for $j = 1, 2, 3$ by

$$v_j = \frac{Det\{\overleftrightarrow{\Delta}_j\}}{Det\{\overleftrightarrow{\mathcal{C}}\}} , \tag{F6}$$

where

$$\overleftrightarrow{\Delta}_1 = \begin{bmatrix} q\tau_1(r_{11}E_1 + r_{12}E_2 + r_{13}E_3) & q\tau_1(r_{13}B_1 - r_{11}B_3) & q\tau_1(r_{11}B_2 - r_{12}B_1) \\ q\tau_2(r_{21}E_1 + r_{22}E_2 + r_{23}E_3) & 1 + q\tau_2(r_{23}B_1 - r_{21}B_3) & q\tau_2(r_{21}B_2 - r_{22}B_1) \\ q\tau_3(r_{31}E_1 + r_{32}E_2 + r_{33}E_3) & q\tau_3(r_{33}B_1 - r_{31}B_3) & 1 + q\tau_3(r_{31}B_2 - r_{32}B_1) \end{bmatrix} , \tag{F7}$$

$$\overleftrightarrow{\Delta}_2 = \begin{bmatrix} 1 + q\tau_1(r_{12}B_3 - r_{13}B_2) & q\tau_1(r_{11}E_1 + r_{12}E_2 + r_{13}E_3) & q\tau_1(r_{11}B_2 - r_{12}B_1) \\ q\tau_2(r_{22}B_3 - r_{23}B_2) & q\tau_2(r_{21}E_1 + r_{22}E_2 + r_{23}E_3) & q\tau_2(r_{21}B_2 - r_{22}B_1) \\ q\tau_3(r_{32}B_3 - r_{33}B_2) & q\tau_3(r_{31}E_1 + r_{32}E_2 + r_{33}E_3) & 1 + q\tau_3(r_{31}B_2 - r_{32}B_1) \end{bmatrix}, \quad (\text{F8})$$

$$\overleftrightarrow{\Delta}_3 = \begin{bmatrix} 1 + q\tau_1(r_{12}B_3 - r_{13}B_2) & q\tau_1(r_{13}B_1 - r_{11}B_3) & q\tau_1(r_{11}E_1 + r_{12}E_2 + r_{13}E_3) \\ q\tau_2(r_{22}B_3 - r_{23}B_2) & 1 + q\tau_2(r_{23}B_1 - r_{21}B_3) & q\tau_2(r_{21}E_1 + r_{22}E_2 + r_{23}E_3) \\ q\tau_3(r_{32}B_3 - r_{33}B_2) & q\tau_3(r_{33}B_1 - r_{31}B_3) & q\tau_3(r_{31}E_1 + r_{32}E_2 + r_{33}E_3) \end{bmatrix}. \quad (\text{F9})$$

By assuming $r_{ij} = 0$ for $i \neq j$, $r_{jj} = 1/m_j^*$ and introducing the notation $\mu_j = q\tau_j/m_j^*$, we find

$$\overleftrightarrow{\mathcal{C}} = \begin{bmatrix} 1 & -\mu_1 B_3 & \mu_1 B_2 \\ \mu_2 B_3 & 1 & -\mu_2 B_1 \\ -\mu_3 B_2 & \mu_3 B_1 & 1 \end{bmatrix}, \quad (\text{F10})$$

$$\overleftrightarrow{\Delta}_1 = \begin{bmatrix} \mu_1 E_1 & -\mu_1 B_3 & \mu_1 B_2 \\ \mu_2 E_2 & 1 & -\mu_2 B_1 \\ \mu_3 E_3 & \mu_3 B_1 & 1 \end{bmatrix}, \quad (\text{F11})$$

$$\overleftrightarrow{\Delta}_2 = \begin{bmatrix} 1 & \mu_1 E_1 & \mu_1 B_2 \\ \mu_2 B_3 & \mu_2 E_2 & -\mu_2 B_1 \\ -\mu_3 B_2 & \mu_3 E_3 & 1 \end{bmatrix}, \quad (\text{F12})$$

$$\overleftrightarrow{\Delta}_3 = \begin{bmatrix} 1 & -\mu_1 B_3 & \mu_1 E_1 \\ \mu_2 B_3 & 1 & \mu_2 E_2 \\ -\mu_3 B_2 & \mu_3 B_1 & \mu_3 E_3 \end{bmatrix}, \quad (\text{F13})$$

and

$$\text{Det}\{\overleftrightarrow{\mathcal{C}}\} = 1 + (B_1^2 \mu_2 \mu_3 + B_2^2 \mu_3 \mu_1 + B_3^2 \mu_1 \mu_2),$$

$$\text{Det}\{\overleftrightarrow{\Delta}_1\} = \mu_1 E_1 + \mu_1 (B_3 E_2 \mu_2 - B_2 E_3 \mu_3) + \mu_1 \mu_2 \mu_3 B_1 (\mathbf{E} \cdot \mathbf{B}),$$

$$\text{Det}\{\overleftrightarrow{\Delta}_2\} = \mu_2 E_2 + \mu_2 (B_1 E_3 \mu_3 - B_3 E_1 \mu_1) + \mu_1 \mu_2 \mu_3 B_2 (\mathbf{E} \cdot \mathbf{B}),$$

$$\text{Det}\{\overset{\leftrightarrow}{\Delta}_3\} = \mu_3 E_3 + \mu_3(B_2 E_1 \mu_1 - B_1 E_2 \mu_2) + \mu_1 \mu_2 \mu_3 B_3 (\mathbf{E} \cdot \mathbf{B}) .$$

For a special case with $\mathbf{B} = \{0, 0, B_3\}$, we get

$$\overset{\leftrightarrow}{\mu}(B_3) = \frac{1}{1 + \mu_1 \mu_2 B_3^2} \begin{bmatrix} \mu_1 & \mu_1 \mu_2 B_3 & 0 \\ -\mu_2 \mu_1 B_3 & \mu_2 & 0 \\ 0 & 0 & \mu_3(1 + \mu_1 \mu_2 B_3^2) \end{bmatrix} . \quad (\text{F14})$$

If we further assume $m_1^* = m_2^* = m_3^* = m^*$ and $\tau_1 = \tau_2 = \tau_3 = \tau_p$, we obtain $\text{Det}\{\overset{\leftrightarrow}{\mathcal{C}}\} = 1 + \mu_0^2 B^2$, $\text{Det}\{\overset{\leftrightarrow}{\Delta}_1\} = -\mu_0 E_1 + \mu_0^2 (B_3 E_2 - B_2 E_3) - \mu_0^3 B_1 (\mathbf{E} \cdot \mathbf{B})$, $\text{Det}\{\overset{\leftrightarrow}{\Delta}_2\} = -\mu_0 E_2 + \mu_0^2 (B_1 E_3 - B_3 E_1) - \mu_0^3 B_2 (\mathbf{E} \cdot \mathbf{B})$, and $\text{Det}\{\overset{\leftrightarrow}{\Delta}_3\} = -\mu_0 E_3 + \mu_0^2 (B_2 E_1 - B_1 E_2) - \mu_0^3 B_3 (\mathbf{E} \cdot \mathbf{B})$, where $\mu_0 = e\tau_p/m^*$. As a result, the mobility tensor $\overset{\leftrightarrow}{\mu}(\mathbf{B})$, which is defined through $\mathbf{v}_d = \overset{\leftrightarrow}{\mu}(\mathbf{B}) \cdot \mathbf{E}$, can be written as

$$\overset{\leftrightarrow}{\mu}(\mathbf{B}) = -\frac{\mu_0}{1 + \mu_0^2 B^2} \begin{bmatrix} 1 + \mu_0^2 B_1^2 & -\mu_0 B_3 + \mu_0^2 B_1 B_2 & \mu_0 B_2 + \mu_0^2 B_1 B_3 \\ \mu_0 B_3 + \mu_0^2 B_2 B_1 & 1 + \mu_0^2 B_2^2 & -\mu_0 B_1 + \mu_0^2 B_2 B_3 \\ -\mu_0 B_2 + \mu_0^2 B_3 B_1 & \mu_0 B_1 + \mu_0^2 B_3 B_2 & 1 + \mu_0^2 B_3^2 \end{bmatrix} , \quad (\text{F15})$$

where $B^2 = B_1^2 + B_2^2 + B_3^2$.

For the surface case with $E_3 = 0$ and $v_3 = 0$, $\overset{\leftrightarrow}{\mathcal{M}}_s^{-1}$, $\overset{\leftrightarrow}{\tau}_{sp}^{-1}$ and $\overset{\leftrightarrow}{\mu}_s(\mathbf{B})$ all reduce to 2×2 tensors.

Appendix G: Bulk and Surface Conductivity Tensors

Under a parallel external electric field $\mathbf{E} = (E_x, E_y, 0)$ and a perpendicular magnetic field $\mathbf{B} = (0, 0, B)$, the total parallel current per length in a p - n junction structure is given by $\int_{-L_A}^{L_D} dz [\mathbf{j}_c^{\parallel}(z) + \mathbf{j}_v^{\parallel}(z)] + \mathbf{j}_s^{\pm}$, where L_D and L_A are the distribution ranges for donors and acceptors, respectively. Here, by using the second-order Boltzmann moment equation, the bulk current densities are found to be⁵

$$\mathbf{j}_{c,v}^{\parallel}(z) = \frac{2e\gamma_{e,h} m_{e,h}^* \tau_{e,h}(z)}{\tau_{p(e,h)}(z)} \mathbf{v}_{c,v}^{\parallel}[u_{c,v}(z)] \{ [\overset{\leftrightarrow}{\mu}_{c,v}^{\parallel}(\mathbf{B}, z) \cdot \mathbf{E}] \} \cdot \mathbf{v}_{c,v}^{\parallel}[u_{c,v}(z)] \mathcal{D}_{c,v}[u_{c,v}(z)] , \quad (\text{G1})$$

where $\mathcal{D}_{c,v}[u_{c,v}(z)] = (\sqrt{u_{c,v}(z)}/4\pi^2) (2m_{e,h}^*/\hbar^2)^{3/2}$ is the electron and hole density-of-states per spin, $u_{c,v}(z) = (\hbar k_F^{e,h})^2/2m_{e,h}^*$ and $k_F^{e,h}$ are Fermi energies and wave vectors in a bulk, $m_{e,h}^*$ are effective masses of electrons and holes, $\tau_{e,h}(z)$ and $\tau_{p(e,h)}(z)$ are bulk energy- and momentum-relaxation times, $\mathbf{v}_{c,v}^{\parallel}(\mathbf{k}) = -\gamma_{e,h} \hbar \mathbf{k}_{\parallel}/m_{e,h}^*$, and $\gamma_{e,h} = -1$ (electrons) and $+1$ (holes), respectively. Similarly, the surface current per length is

$$\mathbf{j}_s^{\pm} = \mp \frac{e\tau_s m_s^*}{\tau_{sp}} \mathbf{v}_s^{\pm}(u_s) \{ [\hat{\boldsymbol{\mu}}_s^{\pm}(\mathbf{B}) \cdot \mathbf{E}] \} \cdot \mathbf{v}_s^{\pm}(u_s) \rho_s(u_s), \quad (\text{G2})$$

where $\rho_s(u_s) = \Delta_0/(2\pi\hbar^2 v_F^2)$ and $u_s = (\hbar k_F^s v_F)^2/2\Delta_0$ are the surface density-of-states and Fermi energy, $k_F^s = \sqrt{4\pi\sigma_s}$, v_F is the Fermi velocity of a Dirac cone, τ_s and τ_{sp} are surface energy- and momentum relaxation times, and $\mathbf{v}_s^{\pm}(\mathbf{k}_{\parallel}) = \pm \hbar v_F^2 \mathbf{k}_{\parallel}/\Delta_0$.

From Eq. (G1), we find the bulk conductivity tensor as

$$\hat{\boldsymbol{\sigma}}_{c,v}^{\parallel}(\mathbf{B}) = e\gamma_{e,h} \int_{-L_A}^{L_D} dz n_{e,h}(z) \left[\frac{\tau_{e,h}(z)}{\tau_{p(e,h)}(z)} \right] \hat{\boldsymbol{\mu}}_{c,v}^{\parallel}(\mathbf{B}, z). \quad (\text{G3})$$

On the other hand, from Eq. (G2) we get the surface conductivity tensor, given by

$$\hat{\boldsymbol{\sigma}}_s^{\pm}(\mathbf{B}) = e\sigma_s \left(\frac{\tau_s}{\tau_{sp}} \right) \hat{\boldsymbol{\mu}}_s^{\pm}(\mathbf{B}). \quad (\text{G4})$$

Therefore, the total conductivity tensor $\hat{\boldsymbol{\sigma}}_{tot}(\mathbf{B}) = \hat{\boldsymbol{\sigma}}_c^{\parallel}(\mathbf{B}) + \hat{\boldsymbol{\sigma}}_v^{\parallel}(\mathbf{B}) + \hat{\boldsymbol{\sigma}}_s^{\pm}(\mathbf{B})$ can be obtained from

$$\begin{aligned} \hat{\boldsymbol{\sigma}}_{tot}(\mathbf{B}) &= e \hat{\boldsymbol{\mu}}_v^{\parallel}(\mathbf{B}) N_A A_h \left[(L_A - W_p) + \int_0^{W_p} dz \exp\left(-\frac{\beta e \bar{\mu}_h N_A}{2\epsilon_0 \epsilon_r D_h} z^2\right) \right] - e \hat{\boldsymbol{\mu}}_c^{\parallel}(\mathbf{B}) N_D A_e \\ &\times \left[(L_D - W_n) + \int_0^{W_n} dz \exp\left(-\frac{\beta e \bar{\mu}_e N_D}{2\epsilon_0 \epsilon_r D_e} z^2\right) \right] + e \hat{\boldsymbol{\mu}}_s^{\pm}(\mathbf{B}) \left(\frac{\alpha_0 \Delta_0}{2\pi \hbar^2 v_F^2} \right) (L_A - L_0) A_s, \end{aligned} \quad (\text{G5})$$

where α_0 and L_0 are constants to be determined experimentally, $N_{D,A}$ are doping concentrations, W_n and W_p are depletion ranges for donors and acceptors in a p - n junction, $\bar{\mu}_{e,h}$ are $\mu_0(z)$ evaluated at $n_{e,h}(z) = N_{D,A}$, $D_{e,h}$ are diffusion coefficients, and $\beta = 4/3$ ($\beta = 7/3$) for longitudinal (Hall) conductivity. In addition, the averaged mobilities $\hat{\boldsymbol{\mu}}_{c,v}^{\parallel}(\mathbf{B})$ are defined by their values of $\tau_{p(e,h)}(z)$ at $n_{e,h}(z) = N_{D,A}$, and three introduced coefficients are $A_s = \tau_s/\tau_{sp} \approx 3/4$,

$$A_{e,h} = \left. \frac{\tau_{e,h}(z)}{\tau_{p(e,h)}(z)} \right|_{n_{e,h}(z)=N_{D,A}}$$

$$= \frac{1}{6} \left(\frac{Q_c}{k_F^{e,h}} \right)^2 \left[2 \ln \left(\frac{2k_F^{e,h}}{Q_c} \right) - 1 \right] = \frac{Q_c^2}{6(3\pi^2 N_{D,A})^{2/3}} \left\{ 2 \ln \left[\frac{2(3\pi^2 N_{D,A})^{1/3}}{Q_c} \right] - 1 \right\}, \quad (\text{G6})$$

where $1/Q_c$ is the Thomas-Fermi screening length.

In addition, the bulk energy-relaxation times $\tau_{e,h}(z)$ are calculated as

$$\begin{aligned} \frac{1}{\tau_{e,h}(z)} &= \left[\frac{2n_i}{n_{e,h}(z)\pi\hbar Q_c^2} \right] \left(\frac{e^2}{\epsilon_0\epsilon_r} \right)^2 \int_0^{k_F^{e,h}(z)} dk \mathcal{D}_{c,v}(\varepsilon_k^{c,v}) \left(\frac{4k^2}{4k^2 + Q_c^2} \right) \\ &= \left[\frac{n_i m_{e,h}^*}{8n_{e,h}(z)\pi^3 \hbar^3 Q_c^2} \right] \left(\frac{e^2}{\epsilon_0\epsilon_r} \right)^2 \left\{ [2k_F^{e,h}(z)]^2 - Q_c^2 \ln \left(\frac{[2k_F^{e,h}(z)]^2 + Q_c^2}{Q_c^2} \right) \right\}, \end{aligned} \quad (\text{G7})$$

and the surface energy-relaxation time τ_s is found to be

$$\frac{1}{\tau_s} = \frac{2\sigma_i}{\pi^2 \sigma_s \hbar^2 v_F} \left(\frac{e^2}{2\epsilon_0\epsilon_r} \right)^2 \int_0^\pi d\phi \int_0^{k_F^s} \frac{k_{\parallel}^2 dk_{\parallel}}{(q_c + 2k_{\parallel} |\cos \phi|)^2}, \quad (\text{G8})$$

where n_i and σ_i are the concentration and surface density of impurities, respectively.

Finally, the bulk chemical potentials for electrons [$u_c(z)$] and holes [$u_v(z)$] are calculated as

$$[u_{c,v}(z)]^{3/2} = 3\pi^2 \left(\frac{\hbar^2}{2m_{e,h}^*} \right)^{3/2} n_{e,h}(z), \quad (\text{G9})$$

and the carrier density functions are

$$n_{e,h}(z) = N_{D,A} \exp \left\{ -\gamma_{e,h} \left(\frac{\bar{\mu}_{e,h}}{D_{e,h}} \right) \left[\Phi(z) + \gamma_{e,h} (E_F^{e,h}/e) \right] \right\}. \quad (\text{G10})$$

Here, the expression for the introduced potential function $\Phi(z)$ is given by

$$\Phi(z) = \begin{cases} -E_F^h/e, & z < -W_p \\ -E_F^h/e + (eN_A/2\epsilon_0\epsilon_r)(z + W_p)^2, & -W_p < z < 0 \\ E_F^e/e - (eN_D/2\epsilon_0\epsilon_r)(W_n - z)^2, & 0 < z < W_n \\ E_F^e/e, & z > W_n \end{cases}, \quad (\text{G11})$$

and E_F^e (E_F^h) is the Fermi energy of electrons (holes) at zero temperature and defined far away from the depletion region.

* d.backes@lboro.ac.uk

† vn237@cam.ac.uk

- ¹ Q. Niu, M.-C. Chang, B. Wu, D. Xiao, and R. Cheng, *Physical Effects of Geometric Phases* (World Scientific Publishing Co. Pte. Ltd., Singapore, 2017).
- ² A. Iurov, G. Gumbs, and D. H. Huang, Phys. Rev. B **98**, 075414 (2018).
- ³ D. H. Huang and M. O. Manasreh, Phys. Rev. B **54**, 2044 (1996).
- ⁴ D. H. Huang, P. M. Alsing, T. Apostolova, and D. A. Cardimona, Phys. Rev. B **71**, 195205 (2005).
- ⁵ D. Backes et al, Phys. Rev. B **96**, 125125 (2017).
- ⁶ X. L. Lei and C. S. Ting, Phys. Rev. B **32**, 1112 (1985).